2013

Design and construction of multi-variable vortex-ring bubble generator for use in interactive exhibit

Hughes, Cale B.

Monterey, California: Naval Postgraduate School

NAVAL POSTGRADUATE SCHOOL

MONTEREY, CALIFORNIA

THESIS

DESIGN AND CONSTRUCTION OF MULTI-VARIABLE VORTEX-RING BUBBLE GENERATOR FOR USE IN INTERACTIVE EXHIBIT

by

Cale B. Hughes

December 2013

Thesis Advisor: Bruce Denardo
Second Reader: Richard Harkins

Approved for public release; distribution is unlimited

THIS PAGE INTENTIONALLY LEFT BLANK

REPORT DOCUMENTATION PAGE			Form Approved OMB No. 0704-0188
Public reporting burden for this collection of information is estimated to average 1 hour per response, including the time for reviewing instruction, searching existing data sources, gathering and maintaining the data needed, and completing and reviewing the collection of information. Send comments regarding this burden estimate or any other aspect of this collection of information, including suggestions for reducing this burden, to Washington headquarters Services, Directorate for Information Operations and Reports, 1215 Jefferson Davis Highway, Suite 1204, Arlington, VA 22202-4302, and to the Office of Management and Budget, Paperwork Reduction Project (0704-0188) Washington DC 20503.			
1. AGENCY USE ONLY *(Leave blank)*	**2. REPORT DATE** December 2013	**3. REPORT TYPE AND DATES COVERED** Master's Thesis	
4. TITLE AND SUBTITLE DESIGN AND CONSTRUCTION OF MULTI-VARIABLE VORTEX-RING BUBBLE GENERATOR FOR USE IN INTERACTIVE EXHIBIT		**5. FUNDING NUMBERS**	
6. AUTHOR(S) Cale B. Hughes			
7. PERFORMING ORGANIZATION NAME(S) AND ADDRESS(ES) Naval Postgraduate School Monterey, CA 93943-5000		**8. PERFORMING ORGANIZATION REPORT NUMBER**	
9. SPONSORING /MONITORING AGENCY NAME(S) AND ADDRESS(ES) N/A		**10. SPONSORING/MONITORING AGENCY REPORT NUMBER**	
11. SUPPLEMENTARY NOTES The views expressed in this thesis are those of the author and do not reflect the official policy or position of the Department of Defense or the U.S. Government. IRB Protocol number ____N/A____.			
12a. DISTRIBUTION / AVAILABILITY STATEMENT Approved for public release; distribution is unlimited		**12b. DISTRIBUTION CODE**	

13. ABSTRACT (maximum 200 words)

The ultimate consequence of the current shortfall of students seeking higher education in the fields of science, technology, engineering and mathematics (STEM) is a lack of technical professionals trained to operate and maintain complex weapon systems crucial to the defense of this nation. A hands-on interactive exhibit able to capture the imagination and ignite curiosity is a powerful tool to advance the strategic goal of raising the number of students studying these disciplines. Vortex rings are a naturally occurring phenomenon that provides a medium for capturing the attention while providing the opportunity to teach complex subjects related to stable and unstable equilibrium, stochastic systems, and conservation laws. The diaphragm valve designed in this thesis provides the centerpiece for such an exhibition. The valve is capable of producing a broad range of vortex-ring bubbles through adjustment of three variables. The seal pressure, actuating pressure, and cycle time of the triggering solenoid valve each contribute to the type and quality of bubble produced. The behavior of the device through a select range of parameters is presented and future work to produce a fully interactive exhibit is discussed, to include mechanical design, electronic circuitry, and micro-controller coding.

14. SUBJECT TERMS Vortex ring bubble, vortex ring, Interactive Exhibit, STEM, diaphragm valve, toroidal ring			**15. NUMBER OF PAGES** 69
			16. PRICE CODE
17. SECURITY CLASSIFICATION OF REPORT Unclassified	**18. SECURITY CLASSIFICATION OF THIS PAGE** Unclassified	**19. SECURITY CLASSIFICATION OF ABSTRACT** Unclassified	**20. LIMITATION OF ABSTRACT** UU

NSN 7540-01-280-5500 Standard Form 298 (Rev. 2-89)
Prescribed by ANSI Std. 239-18

THIS PAGE INTENTIONALLY LEFT BLANK

Approved for public release; distribution is unlimited

DESIGN AND CONSTRUCTION OF MULTI-VARIABLE VORTEX-RING BUBBLE GENERATOR FOR USE IN INTERACTIVE EXHIBIT

Cale B. Hughes
Lieutenant, United States Navy
B.S., Northeastern State University, 2005

Submitted in partial fulfillment of the
requirements for the degree of

MASTER OF SCIENCE IN APPLIED PHYSICS

from the

NAVAL POSTGRADUATE SCHOOL
December 2013

Author: Cale B. Hughes

Approved by: Bruce Denardo
Thesis Advisor

Richard Harkins
Second Reader

Andres Larraza
Chair, Department of Physics

THIS PAGE INTENTIONALLY LEFT BLANK

ABSTRACT

The ultimate consequence of the current shortfall of students seeking higher education in the fields of science, technology, engineering and mathematics (STEM) is a lack of technical professionals trained to operate and maintain complex weapon systems crucial to the defense of this nation. A hands-on interactive exhibit able to capture the imagination and ignite curiosity is a powerful tool to advance the strategic goal of raising the number of students studying these disciplines. Vortex rings are a naturally occurring phenomenon that provides a medium for capturing the attention while providing the opportunity to teach complex subjects related to stable and unstable equilibrium, stochastic systems, and conservation laws. The diaphragm valve designed in this thesis provides the centerpiece for such an exhibition. The valve is capable of producing a broad range of vortex-ring bubbles through adjustment of three variables. The seal pressure, actuating pressure, and cycle time of the triggering solenoid valve each contribute to the type and quality of bubble produced. The behavior of the device through a select range of parameters is presented and future work to produce a fully interactive exhibit is discussed, to include mechanical design, electronic circuitry, and micro-controller coding.

THIS PAGE INTENTIONALLY LEFT BLANK

TABLE OF CONTENTS

THIS PAGE INTENTIONALLY LEFT BLANK

LIST OF FIGURES

ACKNOWLEDGMENTS

The words “look it up” were possibly the most frustrating words my father could utter in response to a question I may have posed. Those words drove me to learn how to use a dictionary, the words made me seek to quench my curiosity in the pages of a book or journal rather than take a quickly dispensed reply as fact. Those words, and the encouragement of my father, have made this work possible. My wife, Stacey, has been my sounding board, my confidante, my rock and my barista. She has shown otherworldly patience, kindness, and understanding

Mr. Steven Jacobs went above and beyond in providing material support and fabrication advice and guidance and assistance throughout the design and fabrication process. Mr. Sam Barone provided the spark with his seemingly endless supply of electronics parts and knowledge.

With one PowerPoint slide, Dr. Bruce Denardo set me on a path to begin this thesis. He has endured my questions, experiments, models, tests, and trials. Dr. Denardo has helped to steady my rudder and navigate the channels and rocky shores. He has brought his considerable knowledge, research, and expertise to bear and helped me form a concept into a design and that design into a readable and accurate work. Dr. Richard Harkins and a little rabbit gave a life and mind to this project that no one else could have supplied. Dr. Andres Larraza has enabled this project to take form and coalesce. With his help, the foundation for the long-term goal of an interactive exhibit is well laid.

THIS PAGE INTENTIONALLY LEFT BLANK

I. INTRODUCTION

A. IMPORTANCE OF SCIENCE, TECHNOLOGY, ENGINEERING, AND MATHEMATICS

This thesis is focused on the design of an interactive demonstration of the development of vortex-ring bubbles. This interactive demonstration will serve to gain the attention of middle-school to high-school age students and fuel their curiosity of science, technology, engineering and mathematics (STEM). The motion of the vortex ring is the draw; the method used to generate the bubble is the hook. Using a combination of mechanical and electronic systems integrated through a programmed microcontroller, users can see the system respond to their input through buttons and dials.

As a child, I visited museums that showcased interactive exhibits that allowed anyone to make changes to a system and observe the resulting changes. This was a turning point of my curiosity and imagination and set the path of study into the sciences. STEM has been identified as a subject of national importance. The United States faces a shortfall of nearly a quarter of a million STEM jobs because Americans are not earning the requisite degrees to fill the positions (Yarros). The May 2010 National Security Strategy highlighted the importance of investment in STEM:

> America's long-term leadership depends on educating and producing future scientists and innovators. We will invest more in STEM education so students can learn to think critically in science, math, engineering, and technology; improve the quality of math and science teaching so American students are no longer outperformed by those in other nations; and expand STEM education and career opportunities for underrepresented groups, including women and girls. We will work with partners—from the private sector and nonprofit organizations to universities—to promote education and careers in science and technology (White House 29).

In response to the goals established by the National Security Strategy, there has been a surge in STEM-related curriculum in schools, websites and other educational resources focused on the important roles that STEM plays in our everyday lives. The US Navy now maintains a Facebook page at https://www.facebook.com/UsNavyStem. The

STEM2Stern Coordination Office at http://www.stem2stern.org works alongside all of the Naval Laboratories and Warfare Centers to maximize the STEM portfolio.

B. GOAL OF HANDS-ON EXHIBIT

Hands-on exhibits serve as a powerful vehicle for ignition, to inspire and nourish an appetite for knowledge and curiosity. This type of exhibition is uniquely suited to meeting the strategic goal of raising the number of American student studying STEM-related disciplines. There are few ways to better emphasize the importance of science, technology and innovation in America's position in the global economy.

Smoke rings rising through the air are an illustration of the most basic of vortex rings in which the ring moves through an identical fluid. Small volumes of dense fluid dropped from a medicine dropper into water will often form vortex rings. In this case, the core fluid is of greater density and viscosity than the surrounding fluid. Vortex rings can be easily produced using simple devices. Producing a vortex-ring bubble, in which the core fluid is both less dense and less viscous than the surrounding fluid is more difficult and stochastic. Hobbs (73) points out that in previous work at the University of Mississippi from 1994–1996, Denardo and Kolaini developed methods capable of 40% formation rates. Thesis work by Hobbs suggested conditions exist for up to 90% formation rates.

Vortex motion is commonly observed in nature and has been an intriguing phenomenon for many centuries. Dust devils on the surface of Mars are essentially small tornadoes or line vortices (Bell). These have been observed to occur in pairs that counter-rotate resulting in translation of the pair. Quantized vortex lines and rings have been observed in superfluid helium (Rief, 116) and Bose-Einstein Condensates (Fitzgerald, 19). In his work *Le Monde, ou Traite de la Lumiere,* Rene Descartes proposed that matter in the universe, from planets to particles moved in such a way that their path could be described as vortex motion. Extensive research in the latter half of the 19th century by prominent physicists such Helmholtz, Kelvin, Thompson and others developed analytical models of vortex motion. Kelvin, notably, even proposed an atomic theory based on vortex rings in the ether (Akhmetov, 4–7). Vortex motion is something that grabs

attention. The motion is violent and symmetric, vicious and beautiful. Vortex rings provide a teaching tool that will both capture the attention of students and provide a real and dynamic demonstration of physical concepts such as stable and unstable equilibrium, stochastic systems, and observable conservation laws.

The challenge posed by this thesis is to develop a method of generating vortex-ring bubbles that allows variation of multiple parameters and can be scaled to increasingly larger devices for potential larger exhibitions in partnership with other Science and Technology Exhibition Centers such as the San Francisco Exploratorium or the San Jose Tech Museum. The parameters of this proposal introduce several problems that were not encountered in previous thesis work by Hobbs in 2000 for the construction and quantification of a toroidal bubble apparatus. How do you protect the system from the potential for damage caused by an untrained user adjusting parameters to values that are either above or below design limits? How do you minimize user interaction with the mechanical aspects of the system while maximizing the variable parameters? Also to consider is the visual appeal; how do you capture the interest and attention of someone passing by? But, the toughest questions were in the device itself: What parameters can be varied to produce a range of behavior? Can it be designed to generate bubbles proportional to the dimensions of the device, independent of other influences like capillary action?

The following chapters discuss the theory and design of a device constructed to serve as the centerpiece of a hands on demonstration for the generation of vortex rings. The next chapter will discuss some of the general theory and equations of motion and conservation. Chapter III presents the proof-of-concept model based on U.S. PAT 7,300,040 B2. Chapter IV gives a detailed description of the prototype device constructed for use in the hands on exhibit. Chapter V explains the testing of the device, observations made and the modifications made to improve the performance of the prototype device. The thesis concludes with chapter VI and the future work to be done with the exhibit.

THIS PAGE INTENTIONALLY LEFT BLANK

II. THEORY

Systematic studies of vortex rings have been conducted since around the middle of the 19th century. These studies began with Helmholtz, who founded the theory of vortex motions of fluids and also carried out a series of experimental observations of vortex ring motion (Akhmentov 2). Experimental observation of vortex rings have shown them to be composed of a toroidal volume of circulating fluid moving in a surrounding medium at an approximately constant translational speed perpendicular to the ring plane. The fluid motion is axisymmetric and the vector of vorticity in the torus is directed along the circles concentric with the circular axis of the torus. A certain volume of the fluid, which embraces the ring and looks like an ellipsoid flattened along the direction of motion, is moving together with the toroidal vortex ring. This enclosed volume of fluid is called the vortex *atmosphere*. Inside the vortex atmosphere the fluid is circulating along the closed streamlines encompassing the toroidal core of the vortex. Motion of the fluid surrounding the vortex resembles the pattern of flow without separation past a corresponding solid body (Akhmentov 22).

A. FUNDAMENTALS

To engage in an analytic approach to the design of a ring generator an understanding of the nature of the bubble must be gained. Figure 1 shows a cross sectional profile of a vortex-ring bubble (Joseph and Wang 1). We will define the parameters with the notation that follows. The cross-section of the air core is considered as the circle of radius b. The air core of the bubble is arranged along a circular axis A having a radius of a from the origin O in the horizontal O-r plane. The bubble translates in the vertical O-z plane. The circulation of the bubble about the axis a is $2\pi\Gamma$.

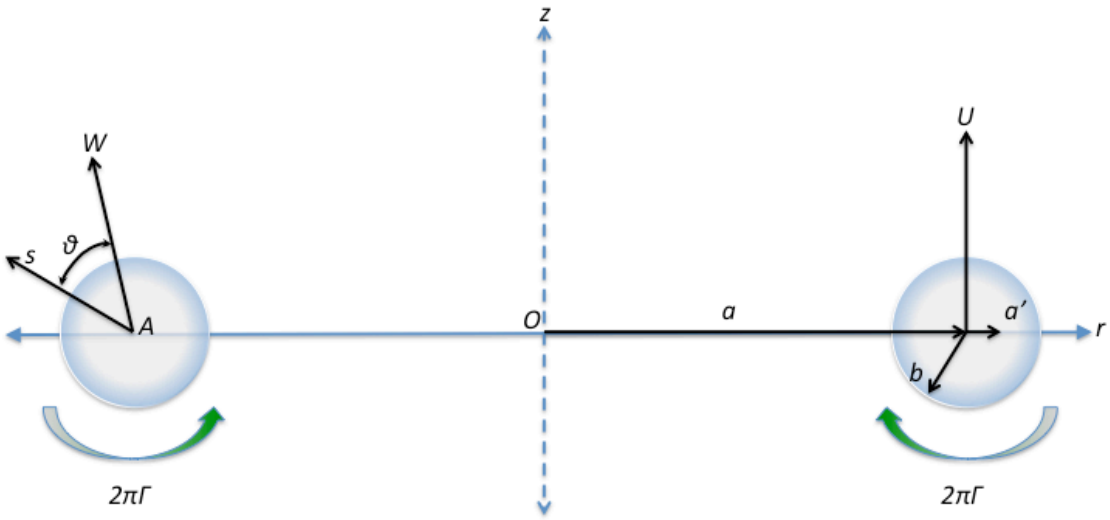

Figure 1. Cross-sectional view of vortex-ring bubble (after Joseph and Wang 1).

From a compilation of analytical studies some of the important relationship can be obtained. The following equations are used to define the volume, circulation, energy and impulse of a vortex-ring bubble. These relationships will be considered in the design of a device for the generation of vortex-ring bubbles. The volume of the bubble can be approximated for conditions when a>>b by the equation (Joseph and Wang, 1):

$$V_b = 2\pi a(\pi b^2)$$

The circulation is a measure of the intensity of the rotation of a vortex. The circulation of a buoyant vortex ring rising in a column of gas can be approximated by the equation (Pedley 98):

$$2\pi\Gamma = 3\sqrt{gV_b}$$

The impulse of a rising vortex-ring bubble that can be approximated by the following equation (Turner 64):

$$P = 2\rho\pi^2\Gamma a^2$$

Because the bubble is traveling a short distance through the water column the change in volume due to the hydrostatic pressure can be neglected. Assume the bubble maintains a constant volume throughout its translation to the surface. The velocity of the

bubble in the vertical direction is given by the expression U. The buoyant forces acting on the bubble give an additional potential energy. As the bubble rises this potential energy adds to the rotational energy. To maintain a constant volume and circulation, then the bubble must necessarily grow in radius a, the rate of horizontal growth of the bubble is given by a′. The translational velocity of the bubble, W, is then given by the equations (Joseph 3, Turner 62, Pedley 101):

$$U = \frac{\Gamma}{2a}\left[\ln\frac{8a}{b} - \frac{1}{2}\right]$$

$$a' = \frac{gV}{4\pi\Gamma a_0}$$

$$W = \sqrt{U^2 + a'^2}$$

With these equations the kinetic energy can be seen as a combination of translational and rotational energy and is approximated by the equation:

$$T = \rho\pi^2 a\left(W^2 b^2 + 2\Gamma^2 \ln\frac{a}{b}\right)$$

B. MOVEMENT OF A VORTEX-RING BUBBLE THROUGH THE WATER COLUMN

The relationship between the radius of the ring bubble and the radius of the vortex atmosphere emerges when the volume of the ring bubble is assumed to be constant due to a relatively short distance of vertical travel and the kinetic energy is assumed to also be constant due to the short time of translation. As the bubble rises through the water column, as shown in Figure 2, the radius expands at the rate a′, the radius of the core decreases to maintain constant volume. As the core radius decreases the rate of rotation increases to maintain circulation constant. As this rate of rotation increases the translational velocity U decreases to maintain constant energy.

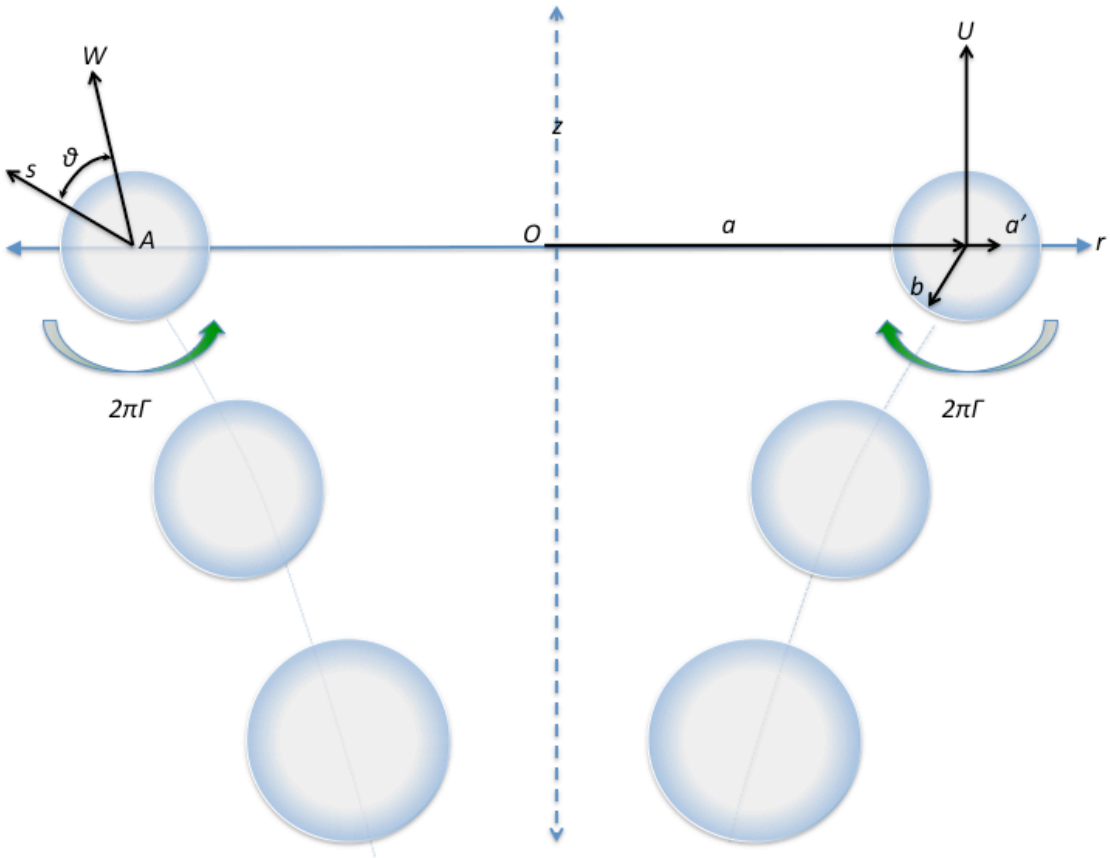

Figure 2. Cross-sectional view of vortex-ring bubble illustrating the effect of expanding radius a of the ring while decreasing the radius b of the core.

C. RELATIONSHIP OF FUNDAMENTALS TO THE DESIGN

What ultimately results from an examination of the equations involved is a relationship between the radius of the vortex b and the size of the ring a. This relationship shows that the behavior of the ring will be most affected by the volume of the bubble produced and the aspect ratio between a and b.

The size of the ring a is related to the size of the orifice in the nozzle being used to produce the bubble and has been shown to be related to the angle at which the nozzle is tapered (Shariff 241–243). The radius of the of the bubble b will be a function of the volume of air used to produce the bubble and as such will be related to a combination of air pressure used to generate the bubble and the amount of time that air is allowed to vent.

A solenoid operated diaphragm valve will allow control over the volume of air initially admitted and the pressure of the air contained in the core of the bubble. Controlling the differential pressure acting across the diaphragm will allow the valve to operate regardless of orientation or static head pressure acting on the device.

THIS PAGE INTENTIONALLY LEFT BLANK

III. PROOF OF CONCEPT

In order to make a practical hands-on demonstration that allows some level of user interaction, a new approach is needed in order to generate vortex rings. An apparatus and method described that allows for the production of vortex-ring bubbles in a liquid (Thomas, 2007) provides a summary of several such devices that use few, if any, moving parts. These devices are similar in design principles and basic concept using the buoyancy of air rising in a column of water to develop the vortex-ring bubble.

A. BACKGROUND

The Thomas device, as shown in Figure 3, is a cylinder. It is open to the surrounding liquid through the lower end and sealed with an endplate on the top to confine a volume of pressurized gas in the upper portion of the cylinder. A short nozzle penetrates the center of the cylinder endplate such that the inlet of the nozzle is at a higher level than the open end of the cylinder. According to Thomas, when pressurized gas is admitted into the cylinder above the nozzles inlet, the liquid is displaced from the cylinder by the confined gas and the liquid level in the cylinder will fall, peeling away from the nozzles open end. The gas will enter the nozzle when the pressure has built up within the cylinder sufficiently to break the liquid surface tension at the nozzle opening. The gas then accelerates up through the nozzle and organizes into a gas filled vortex ring at the nozzle exit. The liquid level in the cylinder rises back up and re-enters the nozzle in a unique self-siphoning action shutting off further gas flow from the nozzle.

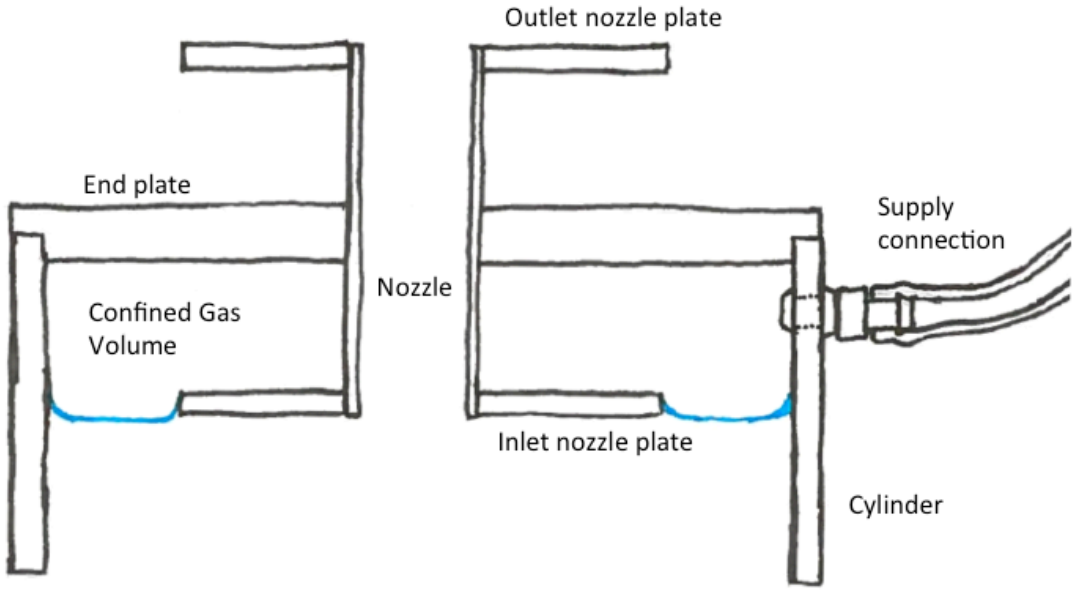

Figure 3. Cross-sectional view of Thomas device showing key components. The light-blue line approximates the curvature of the meniscus.

Although Thomas gives no specific dimensions, in the detailed description of his invention, he briefly discusses the relationship between the length of the nozzle tube, the internal diameter of the cylinder and the distance from the inlet plate of the nozzle tube to the open end of the cylinder. Thomas asserts the governing principles of the operation of the device are described by the following equations:

$$A_m = \sqrt{\frac{L_n}{g}} \quad \text{and} \quad P_m = \frac{\sigma}{R_n},$$

where:

P_m Pressure the meniscus can support
A_m Rate of growth of the meniscus
L_n Length of nozzle
R_n Radius of nozzle
σ Surface tension coefficient
g Gravitational acceleration

Without directly stating, Thomas seems to assert that his device would operate best where the nozzle radius is less than or equal to the radius of the meniscus where the fluid meets the surface of the nozzle.

B. CONSTRUCTION

A model of the Thomas device was constructed to make qualitative observations of the operation of the device. Clear acrylic was chosen to provide visibility of the internal operation and allow for interference fitting of the components. The large thermal expansion coefficient of the acrylic material allows for easy assembly using hot and cold water to fit pieces together. When each component returns to equal temperatures a tightly sealed fit can be achieved without the use of adhesives or other sealants.

An acrylic cylinder with 7.5 in. outer diameter and 0.25 in. wall thickness and height of 6 in. is capped with a 0.5 in thick acrylic endplate. The endplate is 7.5 in. in diameter and has an offset shoulder, as detailed in Figure 4, inset 0.25 in. from the outer edge and 0.25 in. from bottom surface. This shoulder is cut to provide a sealing surface to confine the gas into the cylinder below the endplate. The nozzle is cut from a 1 in. acrylic cylinder, 4 in. in length with a 0.0625 in. wall thickness. The nozzle is inserted into a 1 in. diameter hole centered in the endplate and positioned such that 1.75 in. of the nozzle protrudes above and below the endplate. A 4 in. diameter, 0.25 in. thick acrylic plate is fitted to the inlet and outlet ends of the nozzle. This plate has a 1 in. hole cut in the center to allow the nozzle end to meet flush with the plate surface. These plates provide stabilization of the liquid surface at the inlet and minimize disturbance of the bulk liquid around the outlet of the nozzle. A single hole is drilled through the side of the cylinder 0.75 in. below the sealing surface of the endplate. The hole is threaded to accept a 1/8th in. NPT quick connect hose fitting for the supply gas.

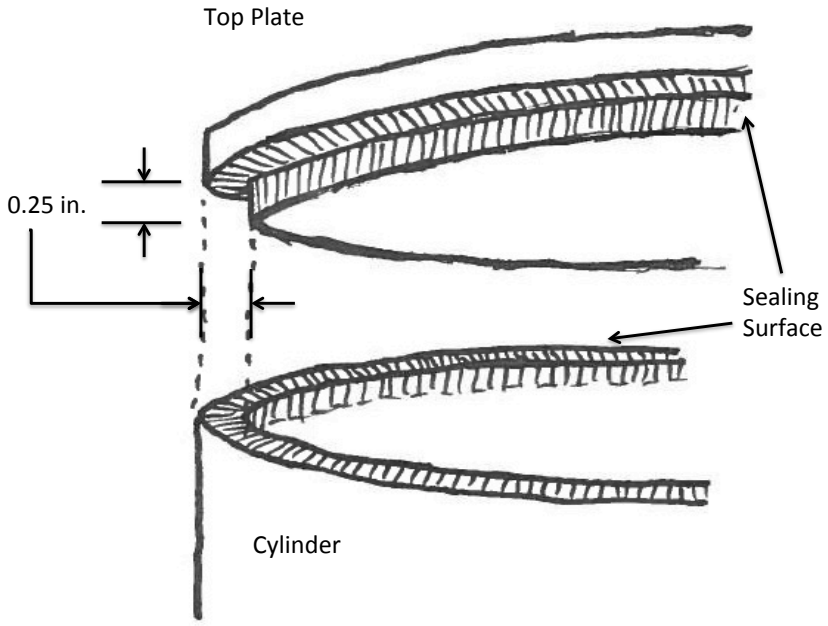

Figure 4. Detail view of endplate shoulder.

A 24 in. diameter weighted base plate is cut from 0.5 in. thick aluminum plate. A 7 in. diameter hole is centered in the plate to accept the open end of the cylinder. Three right angle aluminum brackets 0.75 in. wide are mounted to the base plate 120 degrees apart around the periphery of the center hole. The brackets extend 3 in. above the base plate. Three 4 in. leveling screws are threaded into the baseplate 120 degrees apart and inset 2 in. from the outer edge of the plate. A single fisheye-level bubble is mounted to the surface of the baseplate. The cylinder is inserted into center hole of the base plate. The endplate on the top of the cylinder is leveled relative to the baseplate. A ring-clamp is fitted over the outside of the cylinder and support brackets and tightened snugly to prevent movement of the cylinder. These features can be seen in Figure 5.

Figure 5. Assembled test model on weighted base plate, 1 in. diameter orifice installed. The lower images also show the orientation of the leveling screws and the fisheye-level bubble.

The test model was later modified with an acrylic nozzle tube 2 in. in diameter, 4 in. in length with a 0.25 in. wall thickness. A series of 5 inserts, shown in Figure 6, was made from PVC material 1.50 in. in diameter, 4 in. in length having holes bored through the center successively measuring 0.1875 in., 0.3125 in., 0.4375 in., 0.625 in. and 0.875 in. (3/16, 5/16, 7/16, 5/8 and 7/8) in diameter. This modification was done to qualitatively observe changes in bubble formation using progressively smaller nozzles.

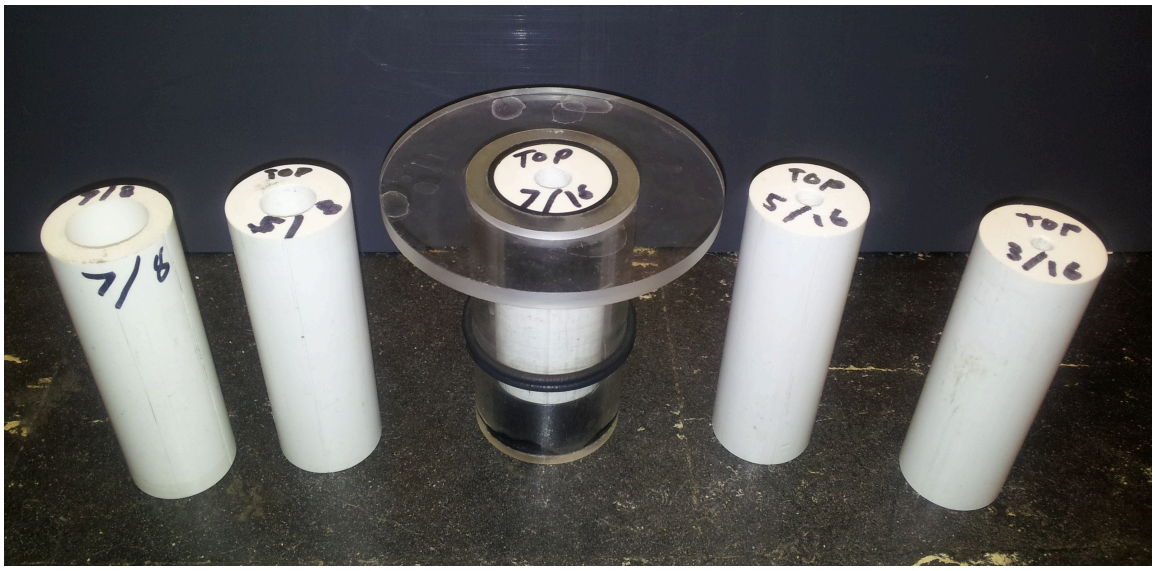

Figure 6. PVC inserts used in test model modification. The 7/16th in. orifice is fitted into the test sleeve. The remaining inserts from left to right are 7/8 in., 5/8 in., 5/16 in., and 3/16- in. diameter nozzles.

Compressed gas was supplied to the test model using dry nitrogen from a compressed gas cylinder through standard regulator to adjust supply pressure. The supply gas is delivered to an intermediate receiver through a high accuracy pressure regulator. The output of the intermediate receiver is connected to the cylinder. The pressure of the cylinder supply gas is measured using a Wallace and Tiernan pressure gauge separately connected to the intermediate receiver. The gauge reads from 0-200 in. of H_2O and is graduated in 0.2 in. increments.

C. TESTING AND OBSERVATIONS

The Thomas model was constructed and initially tested in a steel reinforced glass sided tank. The tank was roughly cubic in construction measuring 36 inches on each side. This tank allowed clear viewing of the displacement of the fluid from the cylinder and of the initial emergence of the burst of air from the top of the nozzle tube. Further testing was performed in a tank measuring approximately 60 in. in depth and of sufficient size to assume there would be no interaction between the bubbles and the tank walls. Each component of the device was cleaned with warm water and mild detergent prior to assembly.

Qualitative results of the testing indicated that supply pressure influences the frequency of the formation of the bubbles, there was no noticeable change in the size of bubbles produced. Fluid displacement from the cylinder was consistent with each cycle measuring approximately 0.35 in. total displacement. From this displacement, the total volume vented during each cycle can be estimated to be approximately 7-8 cubic inches based on diameter of the nozzle tube being used. The inlet plate on the nozzle served to minimize free surface effects as the displaced fluid peeled away from the upper portion and advanced toward the nozzle inlet. The outlet plate minimized turbulence in the water immediately adjacent to the nozzle exit. The initial burst of air, shown in Figure 7, from the exit of the nozzle into the water column did appear to develop vorticity and coalesce into a vortex-ring bubble. Due to time limitations the model as built was not optimized however, after observation of multiple cycles in various configurations, the model of the Thomas design appeared to validate the assertions made in his description.

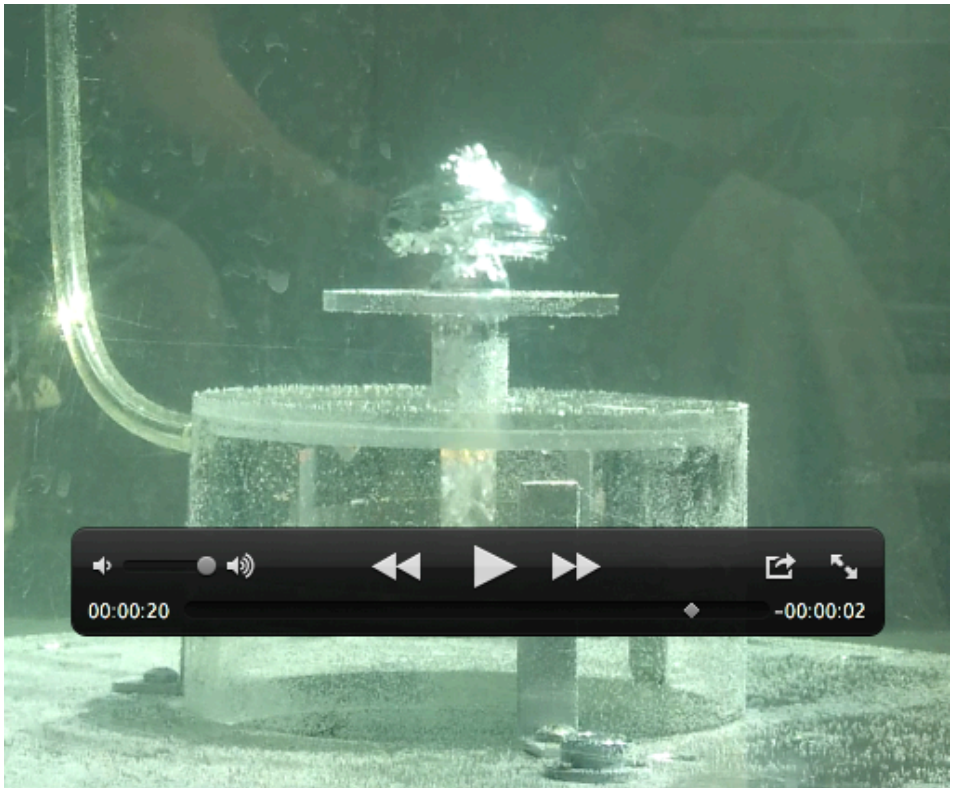

Figure 7. Bubble emerging from nozzle of test model. Bubble spreads and begins to form ring.

THIS PAGE INTENTIONALLY LEFT BLANK

IV. PROTOTYPE

Based on the observations noted in the testing of the Thomas design, the prototype was designed to achieve the following adjustable parameters; seal pressure, actuation pressure, actuating time. The prototype was also designed to operate at up to 90 degrees from the horizontal. The physical construction of the diaphragm valve and nozzle assembly discusses each component individually to provide dimensional information to reproduce each piece. The dimensions are also presented in the diagrams for reference.

A. DIAPHRAGM VALVE AND NOZZLE ASSEMBLY

The diaphragm valve is constructed using acrylic cylinders 2 in. in height and 7.5 in. in diameter with a wall thickness of 0.25 in. for an inner diameter of 7.0 in. The top plate of the actuating chamber and lower plate of the seal chamber as well as the diaphragm flanges were constructed of 0.5 in. thickness acrylic plates. Each portion of the assembly is sealed with O-rings and requires no sealant. 0.5 in. nylon all-thread is used to fasten the entire assembly together.

The seal plate shown in Figure 8 is circular, measuring 10 in. in diameter and is 0.5 in. in thickness. A pattern of 12 0.5 in. holes surrounds the perimeter of the plate. The holes are radially spaced at 30 degrees 4.375 in. from the center of the plate. A seating notch is cut into the upper surface of the plate to provide sealing surfaces for the O-ring seal to mate with the seal chamber cylinder. The notch is 0.25 in. in width and the inner wall of the notch is 3.50 in. from the center of the plate.

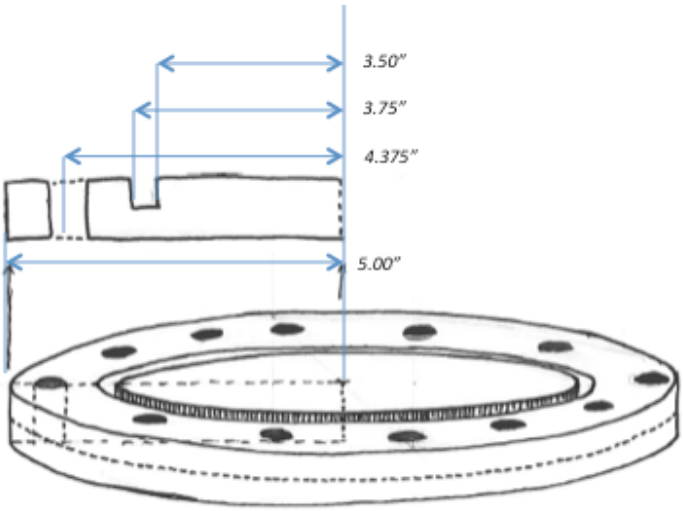

Figure 8. Seal-plate diagram.

The seal flange in figure 7 is also circular, measuring 10 in. in diameter and is 0.5 in. in thickness. A pattern of 12 0.5 in. holes surrounds the perimeter of the plate. The holes are radially spaced at 30 degrees 4.375 in. from the center of the plate. The flange collar is 1.5 in. in width and has a 0.25 in. offset shoulder cut into the lower portion of the inner surface to provide O-ring seating for the mating of the seal chamber cylinder.

The diaphragm is cut from a material that provides a flexible interface between the seal chamber and actuating chamber. The diaphragm provides the sealing surface preventing the backflow of fluid from the nozzle outlet back into the actuating chamber. The diaphragm is cut in a circular pattern 10 in. in diameter and is perforated with the same pattern of 12 holes radially spaced at 30 degrees 4.375 in. from the center as the lower plate and lower flange. The holes in the diaphragm are cut 0.75 in. in diameter. They are larger to allow expansion and contraction of the material and for relative motion between the diaphragm and the flange.

The actuating flange in figure 9 is also circular, measuring 10 in. in diameter and is 0.5 in. in thickness. A pattern of 12 0.5 in. holes surrounds the perimeter of the plate. The holes are radially spaced at 30 degrees 4.375 in. from the center of the plate. The flange collar is 1.5 in. in width and has a 0.25 in. offset shoulder cut into the upper portion of the inner surface to provide O-ring seating for the mating of the actuating chamber cylinder.

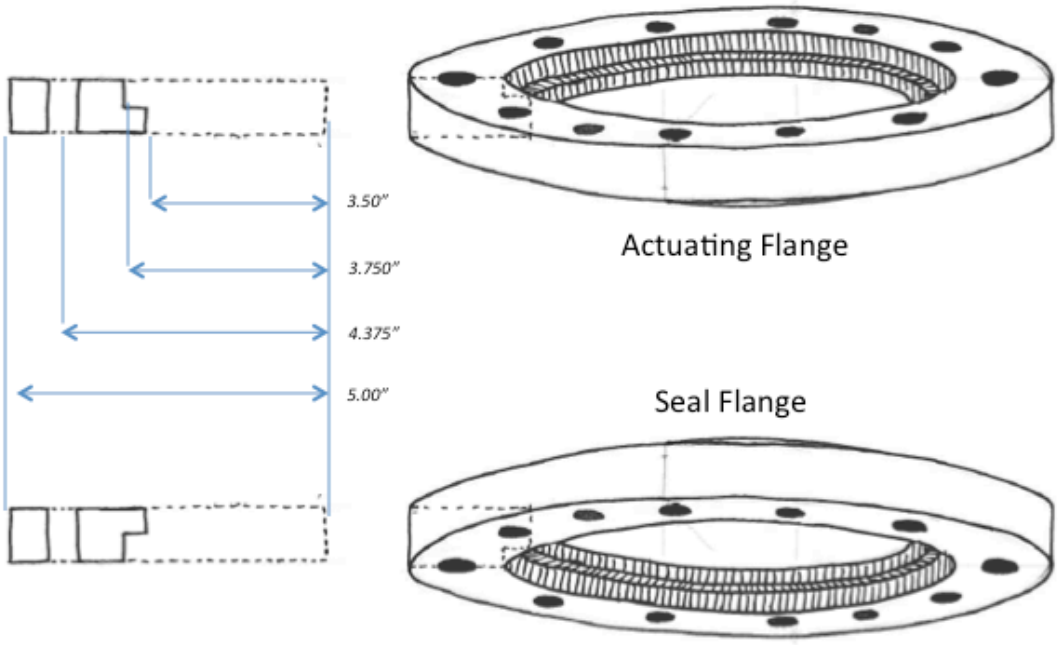

Figure 9. Seal and actuating-flange diagram.

The actuating plate in Figure 10 is circular, measuring 10 in. in diameter and is 0.5 in. in thickness. A pattern of 12 0.5 in. holes surrounds the perimeter of the plate. The holes are radially spaced at 30 degrees 4.375 in. from the center of the plate. A seating notch is cut into the lower surface of the plate to provide sealing surfaces for the O-ring seal to mate with the actuating chamber cylinder. The notch is 0.25 in. in width and the inner wall of the notch is 3.50 in. from the center of the plate. A hole in the center of the plate measuring 1.85 in. in diameter accommodates the nozzle. The center hole is offset with a 2 in. diameter notch cut 0.25 in. deep into the lower surface of the plate. This offset accommodates the nozzle seal O-ring.

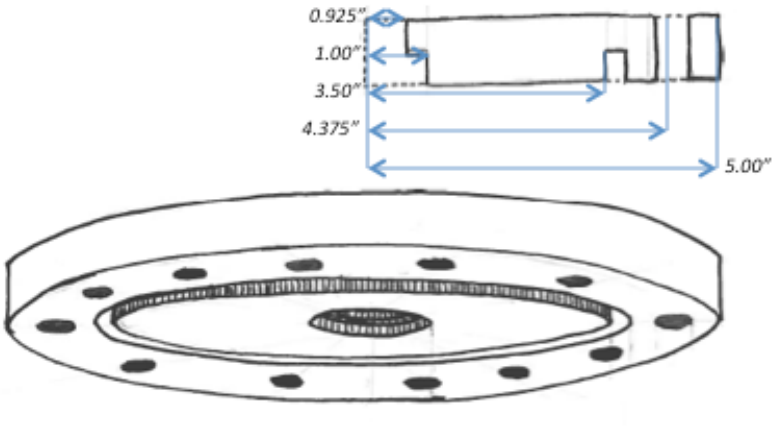

Figure 10. Actuating-plate diagram.

The nozzle in Figure 11 fits into the center hole in the top plate of the actuating chamber and is held in place by friction and the sealing O-ring. The nozzle measures 5.125 in. in length overall and is 2 in. in diameter. The base section of the nozzle is 2.28 in. in height. At that point the nozzle is inset to 1.55 in. diameter this inset is 0.25 in. in height and forms the notch for the nozzle seal O-ring. From this notch the nozzle returns to a diameter of 1.85 in. before beginning to taper at 15-degree angle to a final bore diameter of 0.625 in. The base of the nozzle provides sufficient material to allow for modifications to the seating surface and internal geometry of the nozzle chamber.

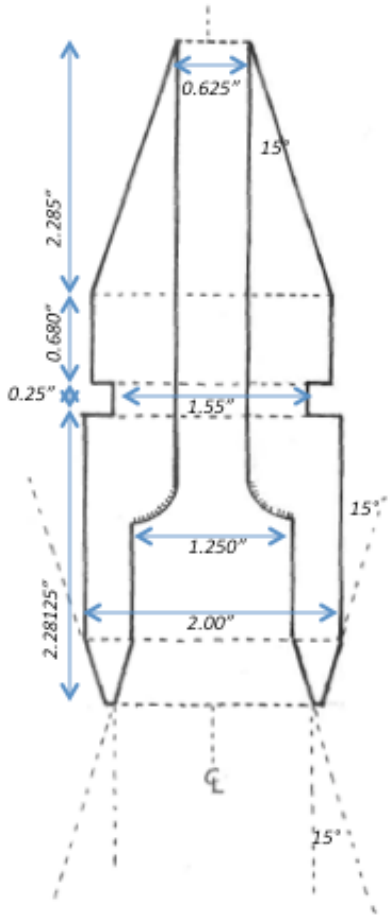

Figure 11. Final dimensions of nozzle based on characteristics described by Akhmetov and Shariff on the formation of vortex rings at a corner and the relationship between the angle of the nozzle and the expansion rate of the bubble radius

The diaphragm valve is assembled as pictured in Figure 12 by passing the all-thread sections, or bolts, through the 12 holes in the lower plate of the sealing chamber. Nuts are threaded onto the end of the bolts. Numbering the bolts in a standard star pattern, the nuts for bolts 1-4 are threaded to leave 4in of threaded bolt below the nuts on the lower plate. This provides sufficient length to attach the diaphragm valve to the weighted base plate used for testing the Thomas device. The remaining bolts, 5-12, are threaded with the nuts remaining flush with the end of the threaded portion. Nuts are threaded onto the bolts with flat washers on the bottom of the lower plate and followed by washers then nuts threaded onto the bolts from the upper end of the bolts. The O-ring is placed onto the sealing surface and the seal chamber cylinder is placed onto the O-ring.

The lower plate may need to be heated using a heat gun to expand the acrylic and allow the fitting of the cylinder into the notch. Nuts are then threaded onto the bolts followed by flat washers. An O-ring is placed onto the seal cylinder and the lower diaphragm flange is lined up and lowered onto the 12 bolts. The flange may more easily line up when heated with heat gun similar to the seal cylinder. The diaphragm is lowered onto the flange and the upper diaphragm flange is lowered onto the bolts. Flat washers and nuts are placed onto the bolts and the nuts are tightened snugly against the flange. It is important that the nuts are not torqued. Place an O-ring onto the sealing surface of the flange and place the actuating cylinder onto the seal. In this case, place the cylinder into the freezer for 10-15 minutes to contract the material to ease the alignment and fit. Nuts are then threaded onto the bolts, followed by flat washers. Place the sealing O-ring onto the nozzle and ensure the O-ring is seated in place. Heat the top plate with a heat gun for 10-15 minutes. Insert the nozzle into the hole in the center of the top plate of the actuating chamber. A leather mallet or dead blow hammer may be used to fully seat the nozzle into the top plate. Align the top plate with bolts and set into place. The final set of flat washers can now be placed onto the bolts and the nuts threaded onto the bolts.

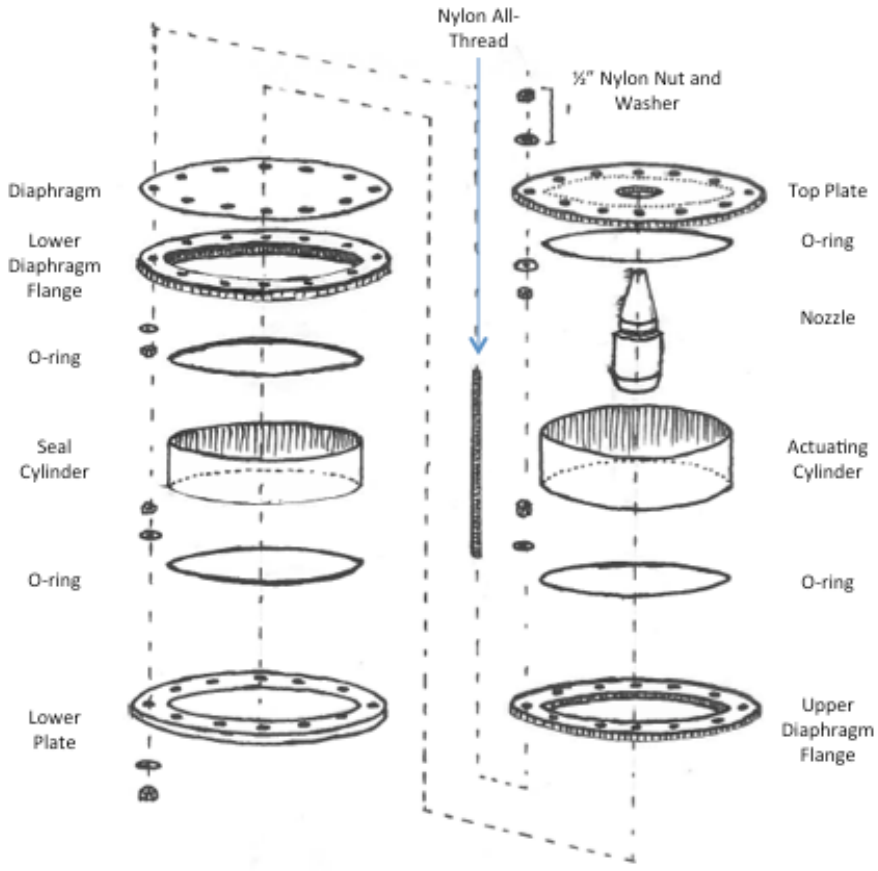

Figure 12. Exploded diagram of nozzle and diaphragm-valve assembly

The nuts are torqued in a standard star pattern, as shown in Figure 13, beginning with the seal flange followed by the actuating flange. The lower nuts of the bottom seal plate are then torqued followed by the upper nuts of the top plate. The nuts interior to the bottom and top plates should remain loose until the flange nuts and outer plate nuts are torqued. The nuts are initially torqued to 20% of the final value, then 40%, 60%, 80% and final torque. For the materials being used the final torque value is 25in-lbs.

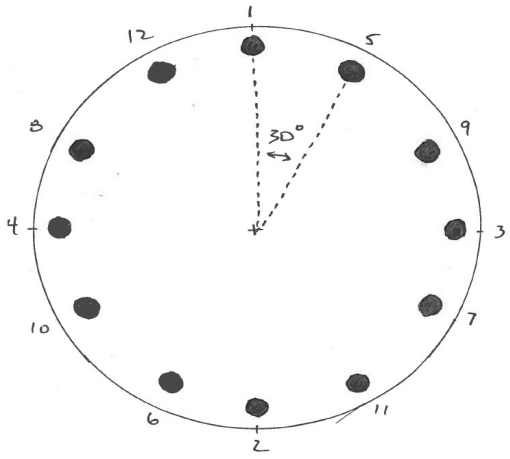

Figure 13. Standard star pattern and bolt numbering used for the assembly and torqueing of the flange nuts for the device. Maximum torque required is 25 in. lbs. and is applied incrementally.

The seal chamber cylinder is tapped between bolt 1 and 12 for a single 1/8th in. NPT to 1/8th in. barb nylon fitting. This fitting will be used to supply pressurized air to the seal chamber. The actuating chamber cylinder is tapped between bolt 1 and 12 for a single 1/2 in. NPT male-to-male copper coupling that will connect to the actuating air system. There is also a tap between bolt 1 and 5 for a single 1/8th in. NPT to 1/8th in. barb nylon fitting to connect to the pressure monitoring system. Threaded connections are wrapped with PTFE tape.

B. AIR PRESSURE CONTROL SYSTEM

The air pressure control system regulates the pressure of supplied compressed air for delivery to the two chambers of the diaphragm valve. The air supplied to the device is provided from any source of compressed air or gas. The proof-of-concept model discussed previously used compressed nitrogen cylinder. The Prototype air system has been designed to receive compressed air from the building low-pressure (LP) compressed air system. The LP air system provides air at nominal 110-psig.

The air system shown in Figure 14 is composed of four air receivers and three pressure regulators. The Storage, Seal and Primary Actuating air tanks are 225 cu. in. and constructed of 4 in. diameter, 18 in. length ABS plastic pipe capped on the ends with 4 in. PVC caps. The Secondary Actuating air tank is 150 cu. in. and constructed of 4 in.

diameter 12 in. length ABS plastic pipe capped on the ends with 4 in. PVC caps. The tanks are sized to minimize pressure transients during actuation of the trigger solenoid valve and to provide a reserve capacity of air to maintain seal pressure in the event of a temporary loss of supply air. The tanks are tapped with 1/8th in. NPT threads for use of barb nylon couplings to attach plastic tubing for connections to supply and control regulators and pressure monitoring systems. The actuating air tanks have additional ½ in. NPT taps for nylon barb couplings. Norgren Space Saver 1/4in 14 standard cubic feet per minute (SCFM) stacked air filter regulators were used for the supply air regulator and both seal and actuating control regulators.

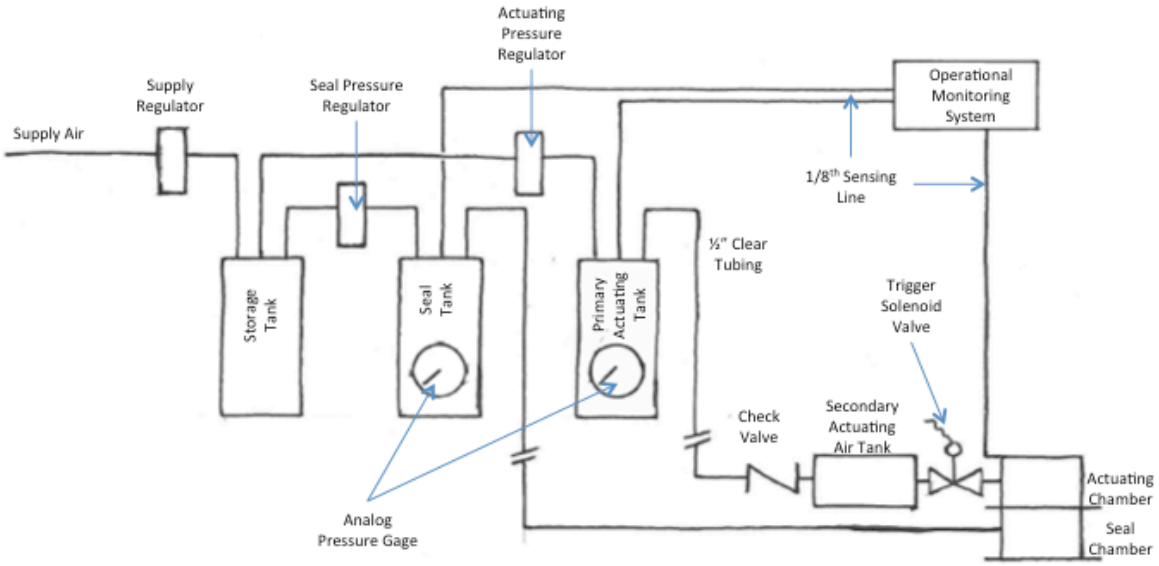

Figure 14. Air system block diagram showing the primary and secondary actuation tanks, seal tank and storage tank, with the analog pressure gages installed on the seal tank and primary actuation tank. The operational monitoring system is included to show the interconnection between systems.

The supply regulator reduces the LP air to 20-psig. The outlet of the supply regulator is connected to the inlet side of the storage tank with 1/8th in. clear plastic tubing. The pressure in the storage tank is maintained low enough to minimize the possibility of damage to downstream components and high enough to assure rapid filling of seal air tank and actuating air tanks. Minimizing the differential pressure across the

seal and actuating air pressure regulators reduces impulse from the rapid transients expected in the actuating air system tank. There are two outlets tapped into the storage air tank. The first outlet connects to the seal pressure control regulator using 1/8th in. clear plastic tubing the second outlet connects to the actuating control pressure regulator.

The seal pressure control regulator delivers regulated air to the seal pressure tank through clear 1/8th in. plastic tubing connected from the outlet side of the regulator to the inlet of the seal air tank. The pressure is set as needed to generate vortex-ring bubbles and maintain the seal between the diaphragm and nozzle to prevent backflow into the actuating chamber. The minimum pressure is determined by height of the static head of water on top of the diaphragm. The maximum pressure is limited to the regulated air available from the storage tank. The seal tank outlet is connected directly to the nylon barb coupling on the inlet of the seal chamber by approximately 20 ft. of 1/8th in. clear plastic tubing.

The actuating pressure control regulator delivers regulated air to the primary actuating air tank through clear 1/8th in. plastic tubing. The pressure is adjusted as needed to generate vortex-ring bubbles. The minimum recommended pressure of the actuating air is the sum of the pressure needed to deflect the seal diaphragm in addition to the seal pressure. There is no minimum actuating pressure required by the design. The maximum pressure is limited to the regulated air available from the storage tank. The primary actuating air tank is connected to a 1/2 in. brass spring loaded check valve on the inlet of the secondary actuating air tank by 20 ft. length of 1/2 in. clear plastic tubing. This check valve provides protection to the upstream components of the actuating air system in the event of a loss of seal pressure. The secondary actuating air tank is connected to the inlet of the triggering solenoid valve using a short section of 1/2 in. clear plastic tubing. 1/2 in. clear plastic tubing is used to reduce the flow losses and decrease the time constant of the pressure transient in the actuating chamber. The outlet of the triggering solenoid valve is directly connected to the actuating chamber using a 2 in. by 1/2 in. NPT male coupling.

C. SOLENOID OPERATED PRESSURE REGULATION

To minimize the possibility for damage to components of the Air Pressure Control System a method of pressure regulation is needed to allow a user to select the desired seal and actuating pressure while preventing them from directly manipulating the pressure regulators. A system was developed using a BL2000 microcontroller in conjunction with the Hewlett Packard Model 726AR DC Power Supply and Kyotto KF0604D Solid State Relay (SSR). Appendix A details the control programming for the pressure control.

Desired seal pressure and actuating pressure (P_{Dseal}/P_{Dact}) is user controlled through the use of voltage divider circuits adjustable from 0.2V-5.2V. The set voltage is detected by the BL2000 microcontroller and compared to the actual seal and actuating reservoir pressures (P_{Aseal}/P_{Aact}) as sensed by the MPX5050 pressure transducers. The BL2000 generates a digital output signal to operate a solid-state relay that switches 24VDC operating voltage to the regulating solenoids of the seal reservoir and primary actuating reservoir. A simplified block diagram is shown in Figure 15.

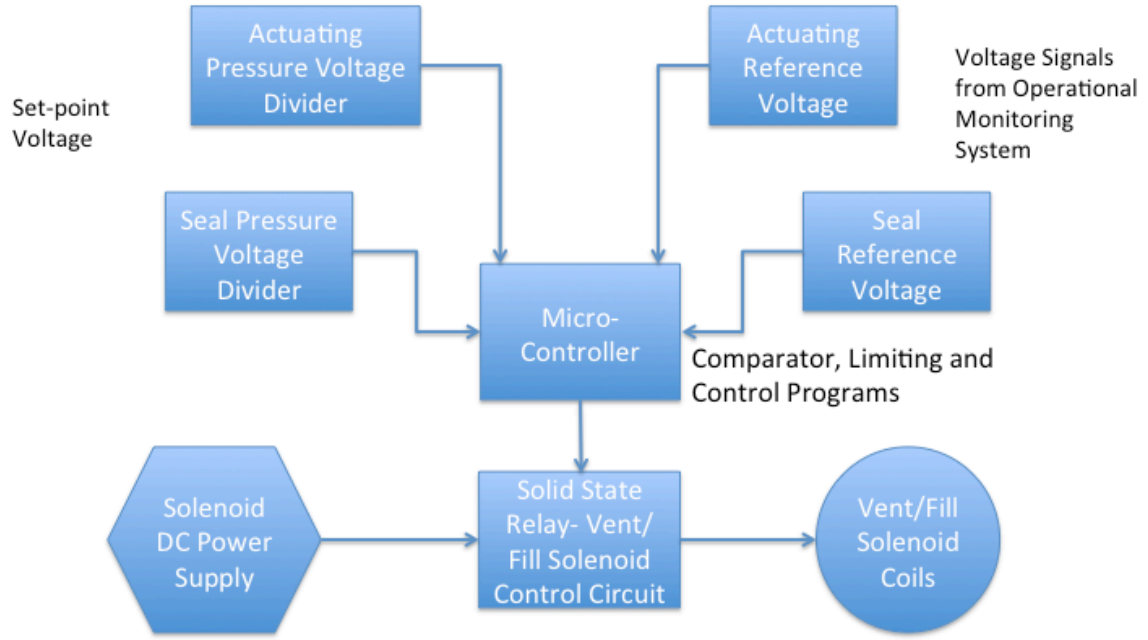

Figure 15. Simplified block diagram showing conceptual solenoid-operated pressure-control system. The set point and reference voltage are from the associated seal- pressure/ actuation-pressure voltage divider and pressure sensors.

Seal pressure and actuating pressure regulation systems operate in similar fashion: If the voltage for the desired pressure setting is higher than the actual voltage from the pressure transducer, indicating the desired pressure is greater than the actual pressure, a digital high signal is passed to the solid state relay controlling the inlet solenoid valve. The inlet valve opens and air is admitted into the reservoir raising the pressure and the corresponding voltage. The digital high signal remains until the desired voltage and actual voltage match to within the tolerance set point. When voltages match, the digital signal goes low, the solid-state relay is switched off and the inlet solenoid is de-energized, closing the inlet valve. Conversely, if the voltage for the desired pressure setting is lower than the actual voltage from the pressure transducer, indicating the desired pressure is less than the actual pressure, a digital high signal is passed to the solid state relay controlling the vent solenoid valve. The vent valve opens and air is released from the reservoir lowering the pressure and the corresponding voltage. The digital high signal remains until the desired voltage and actual voltage match to within the tolerance set point. When voltages match, the digital signal goes low, the solid-state relay is switched off and the vent solenoid is de-energized, closing the inlet valve.

This method of pressure control minimizes user interaction with the physical components of the system and allows limits to be programmed in to prevent the possibility of damage to the air system. The solenoid based design provides the same design functions as the pressure control system described in Chapter III.B.

D. TRIGGER CONTROL SYSTEM

The trigger control system controls the admission of pressurized air into the actuating chamber of the diaphragm valve. The trigger cycle time is analogous to the displacement volume of the test model and will control the size of the bubble produced and to some extent the magnitude of vorticity generated by the diaphragm valve. The trigger control system is capable of cycling the trigger solenoid valve in as little as 8 msec.

The trigger control system, shown in Figure 16, is composed of an Agilent 33220A 20MHz Function Generator/Arbitrary Waveform Generator, Hewlett Packard

Model 726AR DC Power Supply, Kyotto KF0604D Solid State Relay (SSR) control circuit and ASCO Red Hat II 8210G094 1/2 in. high flow solenoid valve.

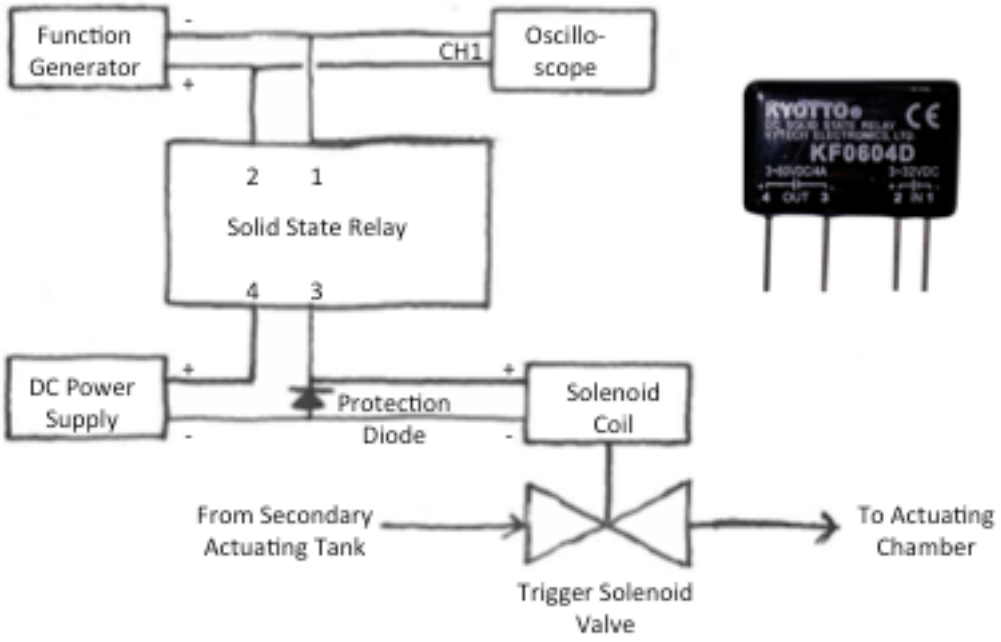

Figure 16. Trigger control-system block diagram. At right is an image of the actual solid-state relay to show pin connections.

The 5 Volt trigger pulse is developed using the pulse mode of the function generator. After selecting the pulse mode, the amplitude is set to 5 peak-to-peak volts with a +2.5 volt DC offset. The pulse width is varied to change the cycle time of the trigger pulse and the period is varied to raise or lower the repetition rate of the pulse cycle.

The SSR has 4 pins. Pins 2 and 1 are the positive and ground pins of the input side of the relay. Pin 4 and 3 are the positive and ground pins on the output (high voltage) side of the relay. The input side of the relay is optically isolated from the output to minimize noise. The function generator output is connected using a BNC to spring hook connector cable. The output lead is connected to pin 2 of the SSR and the ground lead is connected to pin 1. The DC power supply positive output is connected to pin 4 of the solid-state relay. The positive lead of the solenoid valve is connected to pin 3 of the SSR.

Keeping the solenoid valve on the grounded side of the SSR prevents a ground fault in the event of a short circuit in the actuating coil of the solenoid. The ground lead of the solenoid valve is connected to the ground lead of the DC power supply. A protection diode is installed between the positive and negative leads of the solenoid coil to minimize inductive kickback through the circuit.

The 5V pulse from the function generator gates the SSR. When the SSR gates on it completes the circuit to cycle the DC supply voltage to actuate the solenoid valve. A nominal 35 VDC output cycles the solenoid valve to allow operation at cycle times as low as 8 msec. When the solenoid valve cycles, air is admitted into the actuating chamber of the diaphragm valve.

E. MICRO-CONTROLLER BASED TRIGGER CONTROL

The trigger control system can be simplified and integrated into the circuitry used in the solenoid-based pressure regulation system detailed in Chapter III.C using micro-controller logic. The program code in Appendix B details sample code that can be used to generate a 5 volt square-wave pulse of adjustable pulse width and period. This pulse is used in the same way as the trigger pulse generated using the function generator.

The user will adjust the trigger voltage divider on the control panel of the interactive exhibit. The output of the voltage divider is read as an analog input on the BL2000. This voltage is compared to a reference voltage to calculate the delay time for the trigger pulse. The delay time determines the pulse width of the trigger signal. The 5V pulse from the digital output of the micro-controller gates the SSR. When the SSR gates on it completes the circuit to cycle the DC supply voltage to actuate the solenoid valve. A nominal 35 VDC output cycles the solenoid valve. A simplified block diagram of this system is shown in Figure 17.

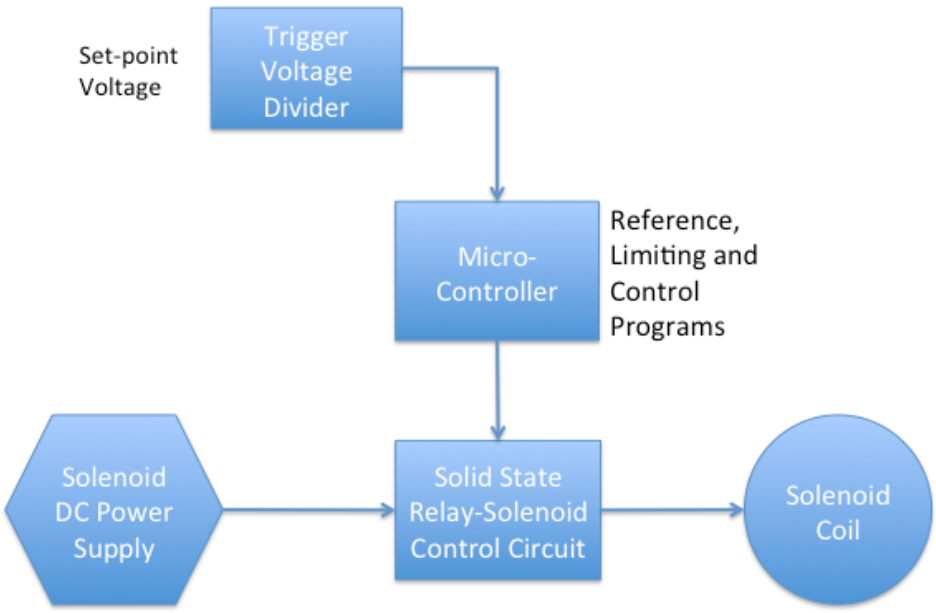

Figure 17. Simplified block diagram for micro-controller-based trigger control. A reference value is given to set the maximum pulse width for each trigger pulse and a minimum wait time between trigger cycles is included to reduce wear and possible damage to trigger solenoid coil and power supply.

The trigger control program contains a set delay time following each trigger cycle to prevent the rapid cycling of the solenoid valve by the user, thereby reducing wear and potential for damage to the solenoid coil and power supply.

F. OPERATIONAL MONITORING SYSTEM

The operational monitoring system in Figure 18 allows for the observation of the parameters of the diaphragm valve and air system and will facilitate the integration of the system into an interactive exhibit. The monitoring system displays the trigger pulse, seal pressure, actuating pressure and the actuating chamber pressure.

4 Freescale Semiconductor MPX5050GP pressure transducers, 2 Ashcroft 0-15-psig pressure gages and Agilent Infiniium PS08064A Oscilloscope make up the operational monitoring system. A Kepco EMR 400K Power Supply is used to provide 5 VDC to the pressure transducers.

The pressure transducers also detailed in Figure 18 are 6 pin uni-body packages. Pin 1 is the output voltage, pin 2 is the ground and pin 3 is +5 VDC supply. Pins 4-6 are

not used. The sensing connection is located in the top of the transducer case and is connected using 1/8th in. blue plastic tubing to the 1/8th in. barb connection of the coupling threaded into the monitored chamber. The transducers are mounted onto a 3M solder less terminal strip and numbered 1-4. The transducers were individually tested for linearity and the output voltage corresponds to 23.5 mV/in. H_2O. The equilibrated voltage is approximately 200 mV. The maximum voltage output is 5.28 V. The expected range of operation of the pressure control system falls between 1.5 V (55 in. H_2O or 1.9-psig) and 5.0 V (204 in. H_2O or 7.1-psig). This range falls within the linear region of the transducers. Transducer 1 was found to have no response below pressures corresponding to approximately 1.3 V. Transducer 1 is connected to the storage air tank, 2 is connected to the seal air tank, 3 is connected to the actuating air tank and transducer 4 is connected to the actuating chamber. Each connection is made using appropriate lengths of 1/8th in. blue plastic tubing.

The design of the operational monitoring system allows it to interface with the microcontroller based pressure control system listed in Chapter III.C and III.E.

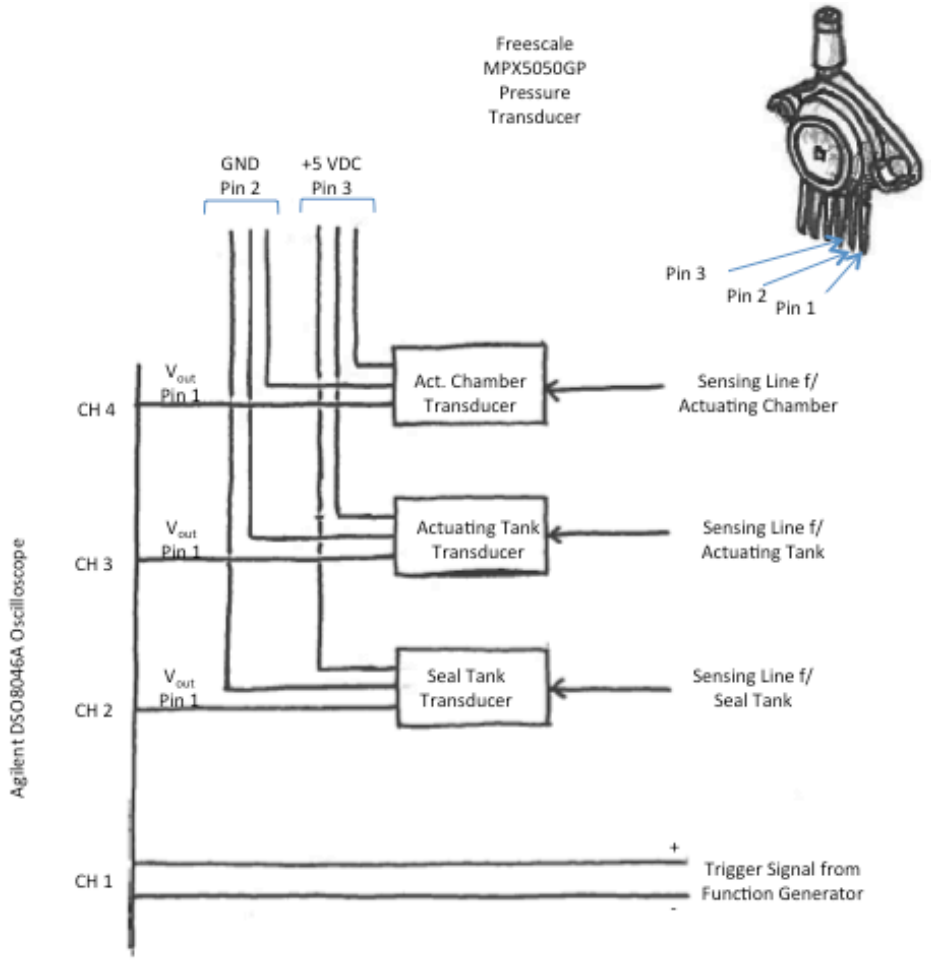

Figure 18. Operational monitoring system connection and block diagram with MPX5050GP detail. The +5VDC and GND are provided from the KEPCO EMR 400K power supply.

During operational cycles the O-scope is set to 200 msec/div and each channel V/div set as needed to display the full waveform. Channel 1 probe is connected to pin 3 of the trigger solenoid SSR to display the actuating signal to the solenoid. Channel 2 probe is connected to the output of transducer 2 to display the seal tank pressure voltage. Channel 3 probe is connected to the output of transducer 3 to display the actuating tank pressure voltage. Channel 4 probe is connected to the output of transducer 4 to display the actuating chamber pressure voltage. The seal and actuating air tanks are additionally monitored using the analog pressure gages listed above.

THIS PAGE INTENTIONALLY LEFT BLANK

V. TESTING, OBSERVATIONS, AND MODIFICATIONS

A. TESTING

Testing consisted of both bench testing and submerged testing performed using the apparatus shown in Figure 19. Bench testing was done to verify the operation of components of the system. Submerged testing of the diaphragm valve was performed in the CAVR pool, located in the lower level of Halligan Hall. This pool is sized such that any boundary effects from the enclosing structure could be ignored. The pool has a depth of approximately 60 in. Given the leveling screws, weighted base plate and mounting bolts, this placed the diaphragm of the valve 52 inches below the surface. This corresponds to a minimum seal pressure voltage of 1,420 mV.

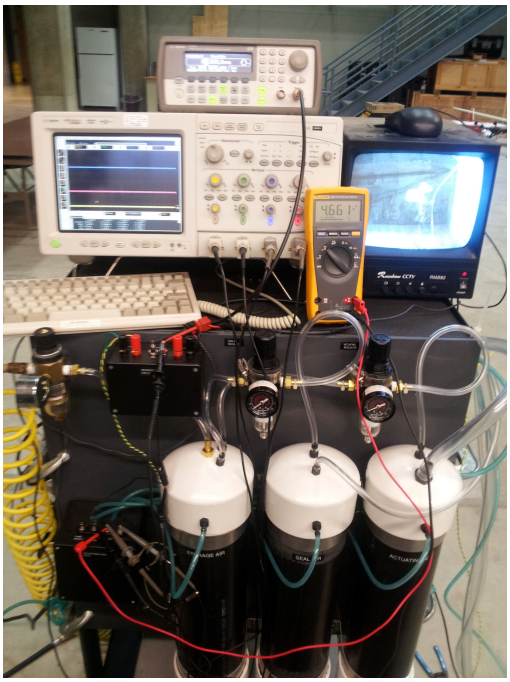

Figure 19. Test apparatus used for bench testing, submerged testing, and qualitative data collection. The monitor in the upper-right portion displays the video feed from a submerged camera, giving an unobstructed view of bubbles emerging from the nozzle and rising to the surface.

Bench testing was performed using the test apparatus. A minimum seal pressure voltage of 400 mV was required to seal the diaphragm to the nozzle seat. Varying seal

and actuating pressures were then applied to observe the minimum cycle time and differential pressure conditions to cycle the diaphragm. This testing also allowed for verification of operations prior to submerged testing.

Qualitative observations were made during testing specifically aimed at determining the relationship between vorticity, translational velocity, vortex size, seal pressure, actuation pressure and cycle time. Three basic conditions of pressure were used to make the observations. The first condition was a low seal pressure with minimum actuation pressure. Minimum actuation pressure is characterized as the actuating pressure required to cycle the diaphragm once for each cycle of the triggering solenoid valve at a cycle time of 10 msec. This condition was met with a seal pressure voltage of 1,650 mV and an actuating pressure voltage of 2,800 mV. The second condition was low seal pressure with high actuating pressure. The seal pressure voltage was maintained at 1,650 mV while the actuating pressure voltage was raised to 5,200 mV. The final condition was a maximum seal pressure with high actuating pressure. Maximum seal pressure is characterized as the seal pressure that allows cycling of the diaphragm once for each cycle of the triggering solenoid valve. Once pressures were established for each of the conditions the cycle time of the triggering solenoid valve was varied from 15 msec up to 100 msec.

Observations made during this testing process were used to determine modifications to be made to the nozzle assembly and actuating air system in order to achieve consistent performance of the device.

B. OBSERVATIONS AND MODIFICATIONS

The spring constant of the diaphragm related to the cycle time of the device. The material selected for the diaphragm must be of sufficient flexibility to allow passage of air past the sealing surface of the nozzle but not so flexible to prevent cycling of the diaphragm at short triggering cycles. The black neoprene diaphragm used during bench testing has a spring constant of approximately 4 kN/m. This diaphragm required a minimum cycle time of 35 msec during bench testing. The red neoprene diaphragm has a

spring constant of approximately 14.7kN/m and can operate at short cycles required for the low seal pressure and 10 msec cycle time.

The original configuration of the actuating air system relied on the primary actuating air tank to supply the actuating chamber. The actuating air passed through approximately 20 ft. of ½ in. clear plastic tubing and the solenoid valve to reach the actuating chamber. The distance traveled coupled with the diameter of the tubing resulted in a large pressure loss to the actuating chamber. This pressure loss presented itself as a slow response to the change in pressure between the actuating cylinder and the actuating chamber. The response time was improved by adding the secondary actuating chamber reducing the distance between the solenoid valve and the pressurized air source. The inclusion of the secondary actuating air tank also allowed for the installation of a check valve into the actuating air system at the inlet to the secondary actuating air tank. This check valve provides protection to the upstream components of the actuating air system in the event of a loss of seal pressure.

The solenoid valve used in the device uses an internally piloted diaphragm for operation. A bleed hole located in the diaphragm shown in Figure 20, allows air from the high-pressure supply to act on the diaphragm to ensure positive seal. When the coil is energized, the slug rises from the diaphragm opening the pilot orifice and vents the bonnet of the valve to the low-pressure side, causing the diaphragm to unseat from the valve and flow proceeds from the supply side of the valve. When the coil is de-energized, the slug drops back to seal the pilot orifice. There is a short time following the actuation of the valve while air vents and the bonnet are pressurized. This venting process was apparent as a steady pressure in the actuating chamber that was slightly higher that the steady state pressure between cycles. This pressure was present for approximately 1.5 seconds following the main airburst of the cycle. During this period a small volume of air slowly bleeds from the valve. This slow flow of air results in a train of bubbles admitting from the nozzle of the device after each actuation of the solenoid valve. To reduce this effect and avoid negatively impacting the operation of the valve the core spring of the valve was replaced with a higher stiffness spring. This modification was effective in

reducing the time the air vented from the device following each cycle of the solenoid valve from approximately 1.5 seconds to approximately 200 milliseconds.

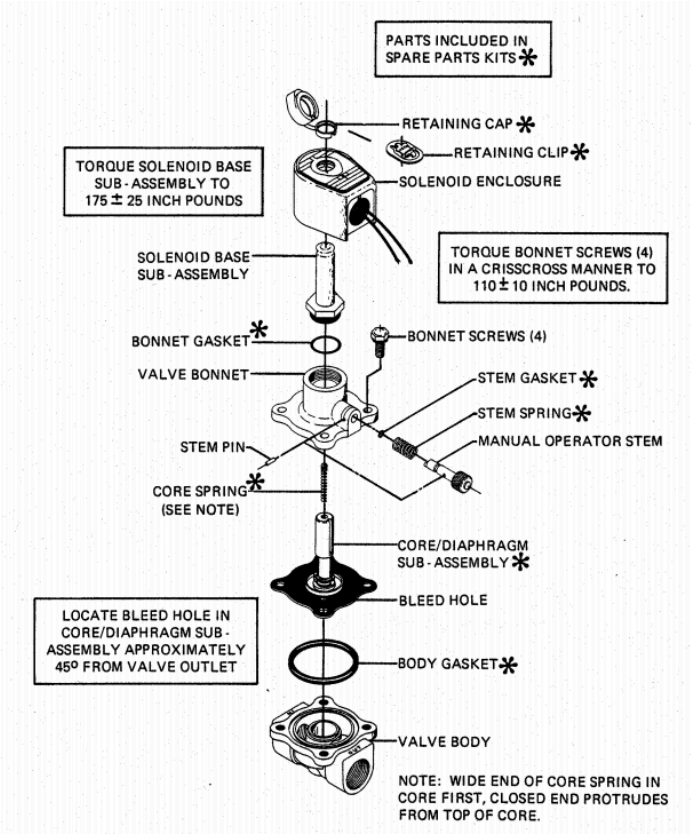

Figure 20. From ASCO form no. V5825R1, showing exploded diagram of ½ in. internally piloted, solenoid-operated diaphragm valve. Of particular interest is the core/diaphragm sub-assembly containing pilot orifice, bleed hole, and core spring.

After initial testing, observation and modification of the device, focus was shifted to the particular characteristics of the rings bubbles being produced. The first bubbles produced in testing were rough and broken in appearance and lacked the anticipated rate of rotation. As cycle times increased above 50 msec. the rings appeared to be composed of several vortices. Based on the appearance of the bubbles and the sound produced during the bench testing this effect was determined to be a result the diaphragm chattering rapidly against the seating surface of the nozzle as shown in Figure 21-A. The base of the nozzle was tapered at 15 degrees from the outer cylinder and the inner portion

of the chamber (Figure 21-B). This reduced the cross section of the seat surface from 0.3125 in. to 0.100 in. This reduction minimized the chattering of the diaphragm while maintaining sufficient seating surface to prevent laceration and excessive wear of the diaphragm. At higher pressure there was leakage of air from the joint between the nozzle and the top plate. A notch was cut into the nozzles top plate seating surface to accommodate a 1/4th in. diameter O-ring to seal the joint (Figure 21-B). The shoulder of the chamber was reduced from 28 degrees to 15 degrees (Figure 21-B to C) and the entire inner surface was polished to smooth the wetted surface. Testing following this modification showed an improvement in the symmetry of the rings produces but reduced the rate of rotation. Using an 80-grit sandpaper to rough the wetted surface produced only slight improvement in rotation rate. A 0.3125 in. radius (Akhmetov 70) was cut into the chamber shoulder with a series of 20 grooves cut to a depth of 0.05 in. spaced evenly across the surface of the shoulder to the nozzle throat. This final nozzle (Figure 21-E) reliably produced vortex-ring bubbles of varying sizes.

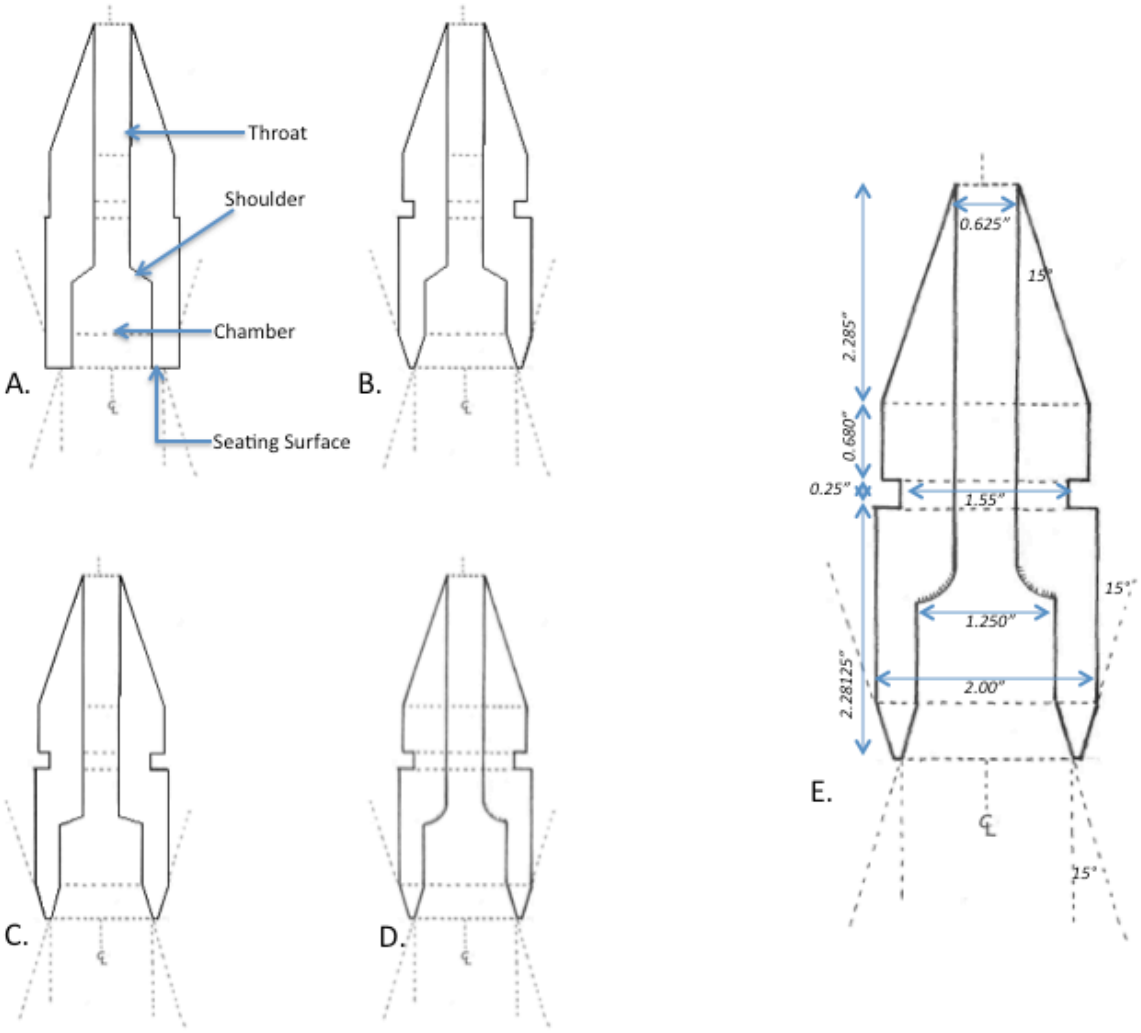

Figure 21. This series of diagrams shows the progressive modifications made to the nozzle assembly. A) Original nozzle assembly with 0.325 in. seating surface. B) First modification to include the O-ring groove to seat to the top plate and the tapered base, reducing the seating surface to 0.100 in. C) Nozzle modified to taper the shoulder portion of the chamber to 15 degrees from 28 degrees and smooth the surface of the shoulder and bore. D) Modification to cut radius into shoulder to provide transition from chamber to bore. E) Final modification to cut axial grooves into the shoulder and rough the wetted surface.

C. QUANTITATIVE OBSERVATIONS

With the modifications completed, a quantitative set of data was gathered to observe the behavior of the device under a range of operating conditions. The conditions used for this testing were the same as those conditions used for the qualitative

observations; a low seal pressure with minimal actuating pressure, low seal pressure with high actuating pressure, and finally the maximum seal pressure with high actuating pressure. A submerged camera allowed for direct observation of the translation, estimation of the size of the bubbles and the height the bubbles travel through the water column before dissipating, or determining whether a bubble indeed forms. The camera is positioned so that the device can be seen at the lowest extent of the field of view and the surface of the pool can be seen in the upper extent of the field of view. The monitor screen is marked with reference points to show the 50 and 75 percent point in the water column and the surface of the water. Reference marks also indicate the horizontal extent of the device to allow for comparison to the size of bubbles produced.

The testing was done beginning with a triggering time of 15 msec. and incrementing by 5 msec. up to 100 msec. The testing was conducted using the three conditions and allowing at least 10 minutes between trigger increments to ensure that any transient effects have stabilized. The tests showed an additional relationship of the vibrational modes of the diaphragm to the probability that a bubble would be produced. Figure 22, 23, and 24 detail the results if the testing under the specified conditions.

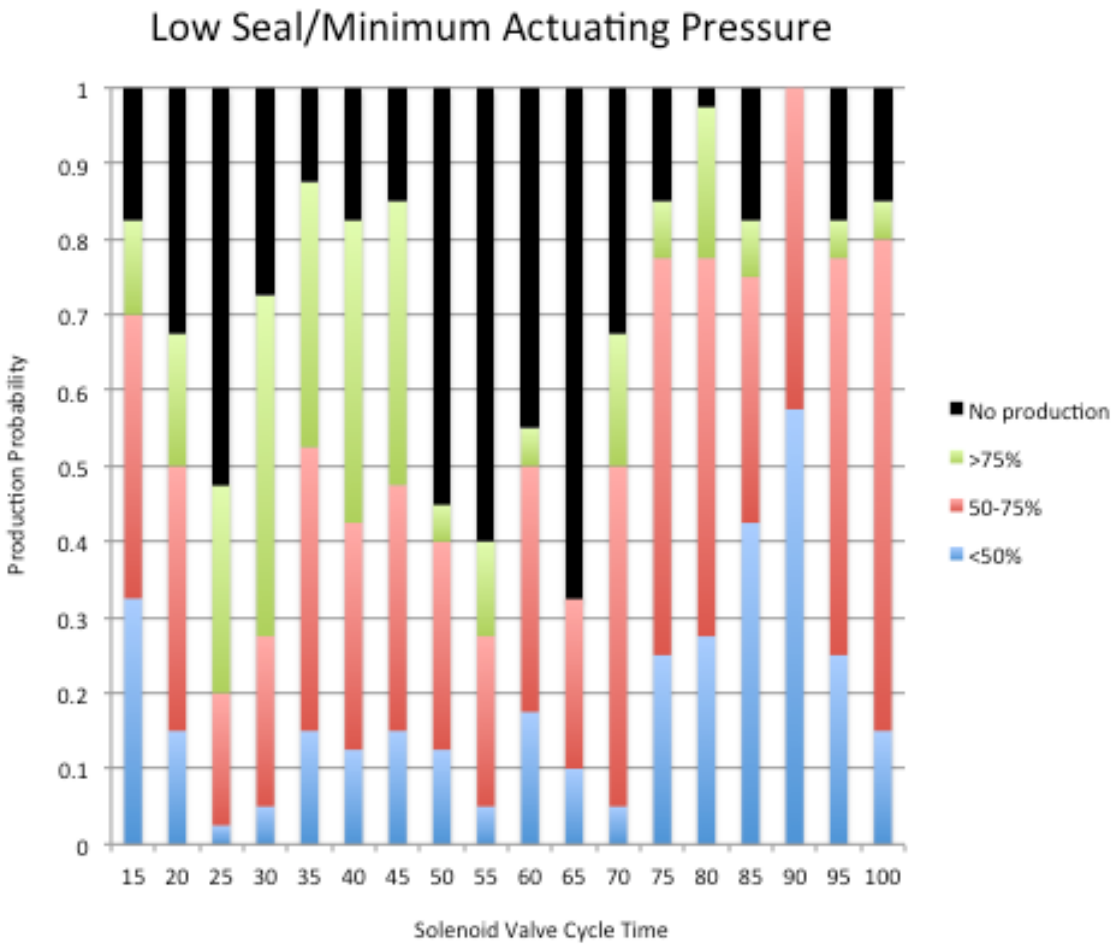

Figure 22. Bar graph illustrating the probability of production of vortex-ring bubble for a seal-pressure voltage of 1650mV and an actuation-pressure voltage of 2800mV. Each time increment consists of 40 individual actuation cycles. Black indicates that no bubble was produced. Blue indicates a bubble was produced, but dissipated before translating above the halfway point. Red indicates the bubble translated between half and three-quarters of the way up the water column. Green indicates the bubble translated greater than three-quarters of the way up the water column.

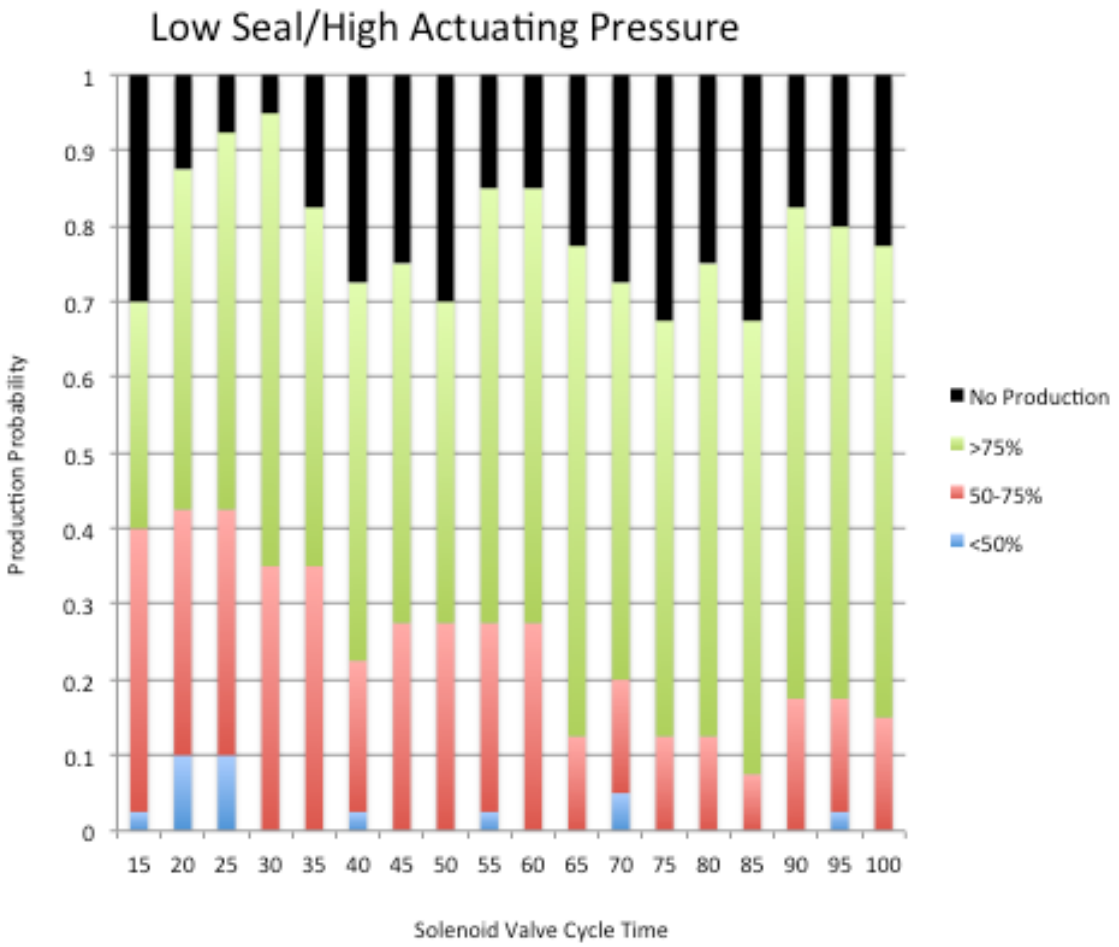

Figure 23. Bar graph illustrating the probability of production of vortex-ring bubble for a seal-pressure voltage of 1650mV and an actuation-pressure voltage of 5050mV. Each time increment consists of 40 individual actuation cycles. Black indicates that no bubble was produced. Blue indicates a bubble was produced, but dissipated before translating above the halfway point. Red indicates the bubble translated between half and three-quarters of the way up the water column. Green indicates the bubble translated greater than three-quarters of the way up the water column.

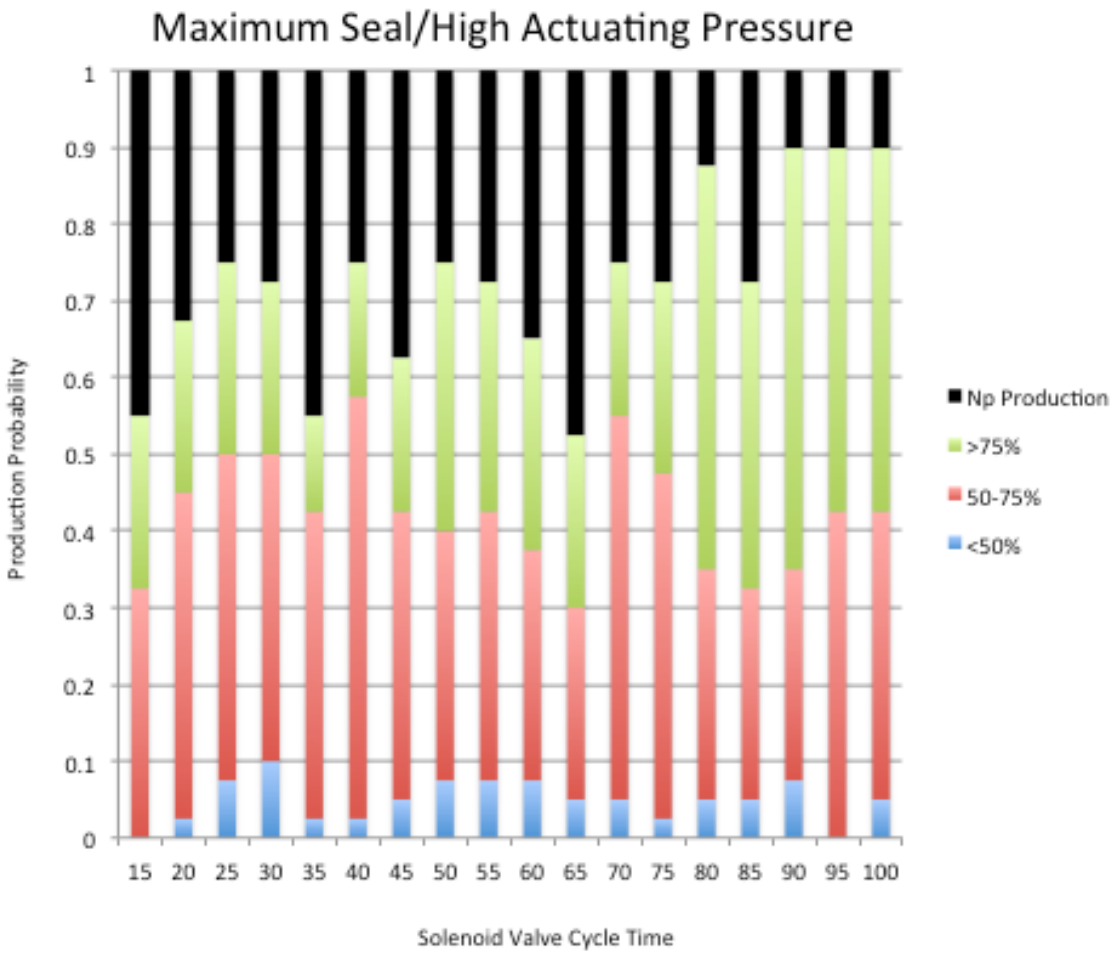

Figure 24. Bar graph illustrating the probability of production of vortex-ring bubble for a seal-pressure voltage of 2440mV and an actuation-pressure voltage of 5050mV. Each time increment consists of 40 individual actuation cycles. Black indicates that no bubble was produced. Blue indicates a bubble was produced, but dissipated before translating above the halfway point. Red indicates the bubble translated between half and three-quarters of the way up the water column. Green indicates the bubble translated greater than three-quarters of the way up the water column.

VI. CONCLUSIONS AND FUTURE WORK

A. MULTI-VARIABLE VORTEX-RING BUBBLE GENERATOR

A device to produce vortex-ring bubbles has been designed and tested and has been shown to produce a variety of bubbles over a range of input conditions. The input parameters can be easily manipulated and the relationship between the input parameters and the performance of the device can be observed. An interesting result of the diaphragm-based design is the effect of symmetrical vibrational modes of the diaphragm on the production of vortex-ring bubbles and the relationship between the vibrational modes and the seal and actuating pressure. The operation of the device provides a real world demonstration of physical concepts and provides an effective medium for capturing the imagination.

While the equations of motion describing the behavior of the bubble accurately approximate the behavior of a vortex-ring bubble after formation, the formation process of the ring bubble remains stochastic in nature. The design contains elements that improve the probability of the formation and achieves formation probabilities in the 90% range.

A solenoid based method of pressure control has been developed to provide a reliable interface between the user and the mechanical components of the device to improve the reliability and durability of the device.

Programming has been developed to produce a 5-volt square wave pulse with an adjustable period based on the input from a voltage divider and read as an analog voltage by a microprocessor. This method allows for the integration of the trigger control routine with the pressure control routine into the same micro-controller as co-states to further simplify the design of the full interactive exhibit.

B. USER INTERFACE

Individual pressure control and trigger control programs developed can be integrated and streamlined to reduce the processing load on the micro-controller. The

user interface can be further improved through the development of Java-based information displays to integrate the output data of the operational monitoring system into the exhibit. The possibility also exists for using touchscreen inputs to adjust the desired input settings pressure and trigger time.

C. CONSTRUCTION OF INTERACTIVE EXHIBIT

The device that has been designed and constructed in this work is the centerpiece of the larger exhibit. The integration of the device into a free-standing interactive exhibit is the next step, requiring the device to be mounted into the bottom of a large acrylic cylinder, and assembled with the required support and interface systems. A space has been designated in the first floor hallway of Spanagel Hall on the Naval Postgraduate School campus and is supplied with a source of compressed air from the building supply air. The design that has been developed can also be enlarged for adaptation to larger venue spaces.

D. DETAILED STUDY OF BUBBLE FORMATION

As noted by Hobbs in 2000 and as witnessed in this work, the actual process of formation of a vortex-ring bubble is difficult to model. This process could be compared to water droplets striking a surface and spreading out, flattening into the circular shape with tendrils extending from the body of the drop. The exact arrangement of those tendrils cannot be modeled but the overall behavior can be approximated. This process is also unpredictable but follows a predictable pattern. Using the exhibit to film high-speed video of the initial formation of the bubble may help in the imaging the initial stages of formation and increase the understanding of the factors that influence bubble formation. This increased understanding could lead to the eventual modeling of the formation process using computational fluid dynamics programs.

APPENDIX A. DYNAMIC-C PROGRAMMING CODE FOR SINGLE CYLINDER PRESSURE CONTROL

The following is an example of the controlling code used for the BL2000 Rabbit micro-controller in a solenoid operated pressure control system. In this example the digital outputs from the micro-controller are labeled as 0, 1 and 2 and relate to the fill, vent and ready signal. The fill and vent signals are 5V outputs from the microcontroller and are of sufficient current and voltage to gate the controlling solid state relay without requiring further control circuitry. This coding can be used as a co-state in a micro-controller based user interface.

```
float DesP, ActP;
int fill, vent, ready;
main(){ //Open Main
//Initialize Board
brdInit();
//Initialize Digital output and variables
digOut(0,0);
digOut(1,0);
digOut(2,0);
fill = 0;
vent = 0;
ready = 0;
while(1){
//Measure and report the analog voltage inputs
        DesP = anaInVolts(0);
        ActP = anaInVolts(1);
//print statements included for troubleshooting code only not required for final.
        printf("Desired Voltage is: %f\t", DesP);
        printf("Actual Voltage is : %f\r", ActP);
//Pressure comparison and adjustment
        if(DesP <= ActP){
                fill = 1;
                printf("\nFill Cylinder\r");
                }else fill = 0;
        if(DesP >= 1.05*ActP){
                vent = 1;
                printf("\nVent Cylinder\r");
                }else vent = 0;
//Pressure adjust and ready
        if(ActP < DesP < 1.05*ActP){
        ready = 1;
        printf("\nReady\r");
        }else ready = 0;
//Digital output and control
        digOut(0,fill);
        digOut(1,vent);
        digOut(2,ready);
        }
}
```

APPENDIX B. DYNAMIC-C PROGRAMMING CODE FOR TRIGGER CONTROL

The following code is a sample program for use in trigger control. The digital output generated by this program approximates a square wave signal pulse of variable width that is determined by the voltage divider input. The program includes a delay to prevent repetitive cycling of the trigger solenoid that could result in damage to the system.

```
float TrigV;
float Vmax;
float PW;
int fire;
//Delay Function
        void msDelay (float sd)
        {
        float t1;
        t1 = MS_TIMER;
                for (t1 = MS_TIMER; MS_TIMER < (sd + t1); );
        }
//Main Function
main(){
        brdInit();
        digOut(0,0);
        Vmax = 7.07;
while(1){
        TrigV = anaInVolts(0);
        //Define the pulse width (PW) of the firing signal to the triggering solenoid
        PW = (TrigV/Vmax)*1000;
                printf("Trigger Voltage: %f\t", TrigV);
                printf("Delay Time: %f\r", PW);
        if(digIn(0)){
                //digital output will be high for the duration of the PW
                digOut(0,1);
                msDelay(PW);
                //digital output is taken low
                digOut(0,0);
                printf("\nFIRE\r");
                //trigger ciruit is locked out for period of milliseconds
                msDelay(1000);
        }else digOut(0,0);
        }
}
```

LIST OF REFERENCES

Akhmetov, D. G., *Vortex Rings.* Verlag, Berlin, Heidelberg: Springer, 2009. Print.

ASCO Valve. *Installation and Maintenance Instructions for 2-way Internal Pilot-operated Solenoid Valves Hung Diaphragm – 3/8, 1/2 and 3/4 NPT Normally Closed Operation Form Number V5825R1.*Florham Park: ASCO Valve. Print

Bell, Trudy E. "The Devils of Mars." *Science@NASA*, July 14, 2013. Web. June 2013

Cullen, James R. "Apparatus for Producing Toroidal Bubbles and Method." Patent 5947784. September 7, 1999. Print.

Fitzgerald, Richard. "An Optical Spoon Stirs Up Vortices in a Bose-Einstein Condensate." *Physics Today* (August 2000): 19–21. Print.

Hobbs, Allen L. *Construction and Quantification of a Toroidal Bubble Apparatus*. MS thesis. Naval Postgraduate School, September 2000. Print.

Joseph, D. D. and J. Wang, *Irrotational Analysis of the Toroidal Bubble in a Viscous Fluid*. University of Minnesota. 2005. Web. June 2013.

Lucey, George K. *Vortex Ring Generator: Mechanical Engineering Design for 100-kpsi Operating Pressures*. Army Research Laboratory, January 2000. Print.

Lundgren, T. S. and N. N. Mansour. "Vortex Ring Bubbles," *Journal of Fluid Mechanics* vol. 224 1991: 177-196. Print.

Pedley, T. J. "The Toroidal Bubble," *Journal of Fluid Mechanics* 32, part 1 1968: 97-112. Print.

Reif, F. "Quantized Vortex Rings in Superfluid Helium." *Scientific American* Dec. 1964: 116–122. Print.

Shariff, Karim and Anthony Leonard, "Vortex Rings." *Annual Review of Fluid Mechanics* 24 1992: 235–279. Print.

Shusser, Michael and Morteza Gharib, "A Model for Vortex Ring Formation in a Starting Buoyant Plume." *Journal of Fluid Mechanics* 416.2000: 173–185. Print.

Takahashi, Masashi and Minoru Yamada, "Method and Apparatus for Producing Vortex Rings of a Gas in a Liquid," Patent 4534914. August 13, 1985. Print.

Thomas, Andrew Sydney Withiel "Simple, Mechanism-Free Device, and Method to Produce Vortex Ring Bubbles in Liquid." Patent 7300040. November 27, 2007. Print.

Turner, J. S. “Buoyant Vortex Rings.” *Proceedings of the Royal Society of London, Series A; Mathematical and Physical Sciences* 239.1216 February 12, 1957: 61–75. Print.

White House, *National Security Strategy,* Washington, DC: May 2010. Print.

Whiteis, David. E. “Apparatus for Creating Vortex Rings in a Fluid Medium.” Patent 2002/0074673 A1. June 20, 2002. Print.

Yarros, Justin. “The STEM Jobs Shortfall is a National Security Shortcoming We Can Fix.” *American Security Project,* April 3, 2013. Web. August 2013.

INITIAL DISTRIBUTION LIST

1. Defense Technical Information Center
   Ft. Belvoir, Virginia

2. Dudley Knox Library
   Naval Postgraduate School
   Monterey, California